

***Design and Realization Methods for  
IIR Multiple Notch Filters and  
High Speed Narrow-Band and Wide-Band Filters***

by

L. Barbara Dai

A Thesis

Presented to the Faculty of Graduate Studies

in Partial Fulfillment of the Requirements

for the Degree

MASTER OF SCIENCE

Department of Electrical and Computer Engineering

University of Manitoba

Winnipeg, Manitoba



National Library  
of Canada

Acquisitions and  
Bibliographic Services

395 Wellington Street  
Ottawa ON K1A 0N4  
Canada

Bibliothèque nationale  
du Canada

Acquisitions et  
services bibliographiques

395, rue Wellington  
Ottawa ON K1A 0N4  
Canada

*Your file* *Votre référence*

*Our file* *Notre référence*

The author has granted a non-exclusive licence allowing the National Library of Canada to reproduce, loan, distribute or sell copies of this thesis in microform, paper or electronic formats.

The author retains ownership of the copyright in this thesis. Neither the thesis nor substantial extracts from it may be printed or otherwise reproduced without the author's permission.

L'auteur a accordé une licence non exclusive permettant à la Bibliothèque nationale du Canada de reproduire, prêter, distribuer ou vendre des copies de cette thèse sous la forme de microfiche/film, de reproduction sur papier ou sur format électronique.

L'auteur conserve la propriété du droit d'auteur qui protège cette thèse. Ni la thèse ni des extraits substantiels de celle-ci ne doivent être imprimés ou autrement reproduits sans son autorisation.

0-612-56117-8

Canada

**THE UNIVERSITY OF MANITOBA  
FACULTY OF GRADUATE STUDIES  
\*\*\*\*\*  
COPYRIGHT PERMISSION PAGE**

**DESIGN AND REALIZATION METHODS FOR IIR MULTIPLE NOTCH FILTERS  
AND HIGH SPEED NARROW-BAND AND WIDE-BAND FILTERS**

**BY**

**L. BARBARA DAI**

**A Thesis/Practicum submitted to the Faculty of Graduate Studies of The University  
of Manitoba in partial fulfilment of the requirements of the degree  
of  
MASTER OF SCIENCE**

**L. BARBARA DAI ©2000**

**Permission has been granted to the Library of The University of Manitoba to lend or sell copies of this thesis/practicum, to the National Library of Canada to microfilm this thesis and to lend or sell copies of the film, and to Dissertations Abstracts International to publish an abstract of this thesis/practicum.**

**The author reserves other publication rights, and neither this thesis/practicum nor extensive extracts from it may be printed or otherwise reproduced without the author's written permission.**

**I hereby declare that I am the sole author of this thesis.**

**I authorize the University of Manitoba to lend this thesis to other institutions or individuals for the purpose of scholarly research.**

**L. Barbara Dai**

**I further authorize the University of Manitoba to reproduce this thesis by photocopying or by other means, in total or in part, at the request of other institutions or individuals for the purpose of scholarly research.**

**L. Barbara Dai**

## ***Acknowledgments***

I would like to express my sincere gratitude to my advisor, Dr. G.O. Martens, for his invaluable guidance, encouragement, and his patience throughout the course of this research. I have greatly benefited from his expertise and constant help and advice, without which this thesis would not have been possible.

I would also like to thank the additional members of the thesis advisory committee, Dr. R. D. Mcleod and Dr. G. B. Scarth, for their valuable suggestions.

Special thanks to my family and friends for their support.

# *Abstract*

In this thesis, a direct IIR design method for real WDFs based on Gazsi's work is summarized in detail, and the cascade realization of first- and second-order allpass sections is generalized to any IIR transfer function, then a simple design method for bireciprocal lattice WDFs is given. A design and realization method for IIR multiple notch filters based on the phase of an allpass filter approximation is described. A design and realization method for high speed narrow-band and wide-band WDFs based on the IFIR technique is given, both nonlinear and approximately linear phase filters are considered; the narrow-band filter is composed of a model filter and one or several masking filters in cascade. In the case of nonlinear phase, conventional lattice and bireciprocal lattice WDFs are used for the model and masking filters; the overall narrow-band filters can be designed by separately designing the model and masking filters. The wide-band filter is composed of a narrow-band filter in parallel with a series of allpass filters, to obtain an overall wide-band filter. The narrow-band filter is designed first, and is then connected in parallel with one of the allpass filters of the narrow-band filter. In the case of approximately linear phase, the linear phase IIR filter is used for the model filter, and a maximum flat linear phase FIR filter is used for the masking filter. Several advantages of these filters over directly designed filters are that they have a substantially higher maximal sample frequency, lower roundoff noise and lower finite wordlength. Several design examples are given to demonstrate the properties of these filters.

# ***Table of contents***

| <b><i>Chapter</i></b>   | <b><i>Page</i></b> |
|---|--------------------|
| <b><i>1. Introduction</i></b> .....   | <b>1</b>           |
| <b><i>2. An IIR design method for real WDF</i></b> .....                              | <b>5</b>           |
| 2.1 Structure of the lattice realization.....   | 5                  |
| 2.2 Realization of lattice WDFs.....  | 10                 |
| 2.2.1 The determination of the multiplier coefficient of a section of degree one..... | 10                 |
| 2.2.2 The determination of the multiplier coefficient of a section of degree two..... | 13                 |
| 2.2.3 Synthesis using cascaded allpass functions.....                                 | 16                 |
| 2.3 Bireciprocal lattice WDF design.....  | 23                 |
| 2.3.1 The definition of bireciprocal filters.....                                     | 23                 |
| 2.3.2 The design method of bireciprocal elliptic filters.....                         | 25                 |
| 2.3.3 The realization structure of bireciprocal elliptic filters.....                 | 25                 |
| <b><i>3. IIR multiple notch filter design</i></b> .....                               | <b>30</b>          |
| 3.1 A multiple notch filter design method.....  | 30                 |
| 3.1.1 Specification transformation.....   | 31                 |
| 3.1.2 The structure of the lattice realization.....                                   | 38                 |

|   |           |
|---|-----------|
| 3.1.2.1 The determination of the allpass filter coefficients..... | 38        |
| 3.1.2.2 Lattice realization structure.....                        | 39        |
| 3.2 The design procedure and an example.....                      | 41        |
| 3.2.1 Summary of design procedure.....                            | 41        |
| 3.2.2 The design example.....                                     | 42        |
| <b>4. High speed narrow-band and wide-band filter design.....</b> | <b>46</b> |
| 4.1 The interpolated FIR (IFIR) method.....                       | 46        |
| 4.2 Nonlinear phase narrow-band and wide-band filter design.....  | 49        |
| 4.2.1 Nonlinear phase narrow-band filter design.....              | 49        |
| . Maximal sample frequency analysis.....                          | 50        |
| . Narrow-band filter structure.....                               | 52        |
| . Design of narrow-band lowpass filter.....                       | 53        |
| . Summary of design procedure.....                                | 56        |
| 4.2.2 Nonlinear phase wide-band filter design.....                | 56        |
| 4.3 Linear phase narrow-band and wide-band filter design.....     | 59        |
| 4.3.1 Linear phase narrow-band filter design.....                 | 59        |
| . Model filter design.....  | 59        |
| . Masking filter design.....                                      | 63        |
| 4.3.2 Linear phase wide-band filter design.....                   | 63        |
| 4.4 Roundoff noise analysis for interpolated WDFs.....            | 64        |
| 4.5 The examples.....   | 65        |



|   |     |
|---|-----|
| <b>5. Conclusions</b> .....                     | 88  |
| <b>Appendix</b> .....                           | 90  |
| 1. Programs for the multiple notch filters..... | 90  |
| 2. Programs for the wide-band filters.....      | 94  |
| <b>References</b> .....                         | 103 |

# ***Chapter 1***

## ***Introduction***

A design and realization method for IIR (infinite impulse response) multiple notch filters is described. A notch filter is a filter which has a single or very narrow rejection band extending from a finite lower cutoff frequency to a finite upper cutoff frequency. Frequencies within the rejection band are eliminated or attenuated while frequencies outside the rejection band are passed. Notch filters have a wide variety of applications in the field of signal processing for removing a single frequencies or a narrow-band of sinusoidal interference. Multiple notch filters are used for the removal of multiple narrow-band or multiple frequency interference. When the frequencies of narrow-band interferences are known in advance, fixed notch filters can be used. We will focus on the fixed IIR notch filter design problem, and use the method which is based on the phase of allpass filter approximation. A more detailed derivation for the approach and lattice implementation will be presented than in [15].

Digital filters can only be implemented with finite precision arithmetic, thus the filter coefficients must be approximated. Errors, such as rounding errors and overflow can arise from coefficient and signal quantization. It is well know [31] that IIR lattice wave digital filters have low passband sensitivity and low level rounding noise to coefficient quantiza-

tions. In addition, they have good stability properties even under nonlinear operating conditions resulting from overflow and roundoff effects. We refer to the review paper by Fettweis [31] and the references contained therein for a detailed discussion of WDFs (wave digital filters) and their advantages.

There are many different possible structures for WDF realizations of the classical reference filters. Gazsi [6] presented a direct design method for real lattice WDFs where both lattice branches are realized by cascaded first- and second-degree allpass sections. This method makes the design process direct and simple.

However, for narrow-band and wide-band filters, high sensitivity problems occur even with this type of realization since most of the poles are very close to the unit circle.

In this thesis, based on the IFIR (interpolated finite impulse response) technique [18] and [19], a design and realization method for high speed narrow-band and wide-band filters is presented. For nonlinear phase, conventional lattice WDFs are used for the model filters, and bireciprocal lattice WDFs are used for the masking filters. Since a bireciprocal elliptic filter is a special case of a elliptic filter, it is possible to modify any standard elliptic filter algorithm such that the definition of bireciprocal elliptic filters is satisfied. The advantage of using lattice WDFs is that they make it possible to obtain stable filter algorithms under finite-arithmetic conditions [31]. The IFIR technique was introduced in order to reduce the complexity of FIR filters with a narrow transition band. It was later used in [30] where an IIR filter is used for the model filter, whereas FIR filters are used for the masking filters. One advantage of using the IFIR technique is that the poles of the recursive model filter are closer to the origin compared with the poles of the directly designed filters, and this will lower the roundoff noise [32]. Furthermore, the model and masking

filters can be realized in many different ways, which offers the possibility of using structures that have good properties under finite-arithmetic conditions, and that are well suited for implementation in hardware. The major advantage of using the interpolated technique is that the new filters have higher maximal sample frequency compared with the directly designed filters, this is important for high speed low power portable applications. It should be pointed out that we give the entire design and realization procedures compared with [20], the main purpose of that paper [20] was to present the realization structure, and we give a lattice bireciprocal approach which is simple and easy to design, we also indicate how to choose the maximum interpolated value for a model filter. For the case of linear phase, we also give the more detailed design method compared with [25].

In Chapter 2, we briefly describe the IIR real WDFs in the lattice structure and the method used in [6] to realize odd-order classical filters. The implementations of first- and second-degree allpass sections by means of three-port circulators will be presented in detail, and the realization method will be generalized to any IIR transfer function. And a design method for bireciprocal elliptic WDFs will be formulated.

In Chapter 3, the design and realization method for IIR multiple notch filters will be presented. First, we transform the specification of a notch filter into that of an allpass filter. As a result, the notch filter design problem becomes an allpass filter design problem. Second, we will develop an approach to determine the allpass filter coefficients, and the lattice realization will be presented. Then, we will summarize the entire design and realization procedures in detail, an example will be given to demonstrate the procedure.

In Chapter 4, we will first describe the IFIR technique, analyze the maximal sample frequency for different lattice WDF structures, then, we will present the design and realiza-

tion procedures for narrow-band and wide-band filters, we will use the method described in Chapter 2 to design the individual model and masking filters, roundoff noise will be discussed, several examples will be given, and in Chapter 5 the conclusions.

# ***Chapter 2***

## ***An IIR design method for real WDFs***

The approximation problem in general analog filters (such as Butterworth, Chebyshev, Inverse-Chebyshev, Elliptic (Cauer)) has been a subject of research throughout the past sixty years, and some powerful methods have been developed for its solution [1-5] and [7]. These methods yield a complete description of the continuous-time transfer function in closed form, either in terms of its zeros and poles or its coefficients. The main purpose of this chapter is to describe the lattice wave digital filter realization by using the existing theory of analog filter design and a generalization of the basic theory in [6]. In [6], a direct design method is given for lattice WDFs, where both lattice branches are realized by cascaded first- and second-degree allpass sections (see section 2.2). In section 2.3, a design method of birciprocal elliptic filters by modifying standard elliptic filters is presented. Examples which demonstrate the above procedures are given.

### **2.1 Structure of the lattice wave digital filters**

WDFs were first introduced as a method of mapping a lossless analog filter (known as the reference filter) to a digital filter using voltage wave quantities [8]. There were two motivations for this:

1. WDFs inherit the low passband coefficient sensitivity of doubly-terminated lossless analog filters.

2. The procedure allows the use of the existing theory of analog filter design to derive the reference filters, which then can be mapped to the corresponding WDF.

Consider a two-port (Figure 2.1) where for port  $i$  ( $i = 1$  or  $2$ ), the voltage is  $V_i$ , the current  $I_i$ , and the port (or normalizing) resistance  $R_i$ .

Then the analog signal variables  $V_i$  and current  $I_i$  can be mapped to the incident and reflected wave quantities  $A_i$  and  $B_i$  by

$$A_i = V_i + R_i I_i, \quad B_i = V_i - R_i I_i, \quad i = 1, 2 \quad (2.1a)$$

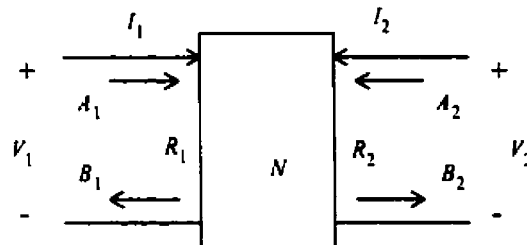


Fig. 2.1 A two-port  $N$  with port resistances  $R_1$  and  $R_2$ .

and

$$\mathbf{a} = \begin{bmatrix} A_1 \\ A_2 \end{bmatrix} \quad \mathbf{b} = \begin{bmatrix} B_1 \\ B_2 \end{bmatrix} \quad (2.1b)$$

The incident and reflected wave vectors are related by the scattering equation [9]

$$\mathbf{b} = \mathbf{S}\mathbf{a} \quad (2.2)$$

where  $\mathbf{S}$  is called the scattering matrix:

$$\mathbf{S} = \begin{bmatrix} s_{11} & s_{12} \\ s_{21} & s_{22} \end{bmatrix} \quad (2.3)$$

we let that the two-port be symmetric and reciprocal, i.e.

$$s_{11} = s_{22}, \quad s_{12} = s_{21} \quad (2.4)$$

Next, define reflections  $S_1 = s_{11} - s_{21}$ ,  $S_2 = s_{11} + s_{21}$  and take (2.4) into account. In

view of (2.1b) and (2.3), (2.2) can be written as

$$2B_1 = S_1 (A_1 - A_2) + S_2 (A_1 + A_2) \quad (2.5a)$$

$$2B_2 = -S_1 (A_1 - A_2) + S_2 (A_1 + A_2) \quad (2.5b)$$

These equations lead to the lattice realization of a WDF shown in the following Fig.2.2(a).

For  $A_2 = 0$  and disregarding  $B_1$ , the above signal-flow diagram simplifies to Fig. 2.2(b).

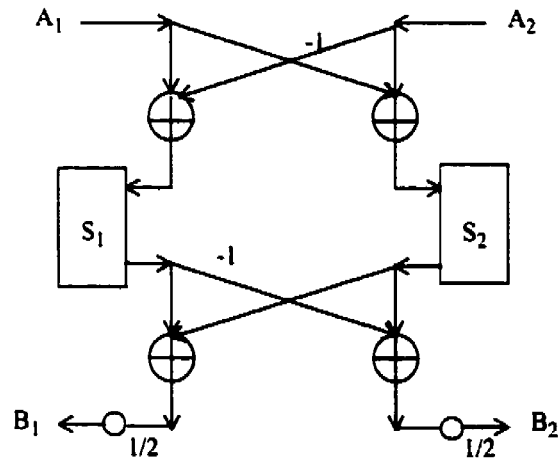


Fig. 2.2 (a) Signal-flow diagram of a lattice structure.



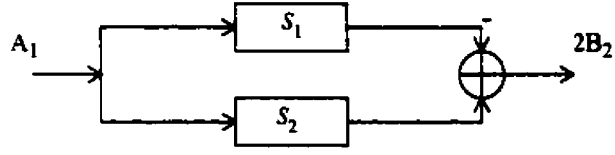


Fig. 2.2 (b) Simplified wave-flow diagram.

Therefore the realization reduces to the realization of two reflectances:  $S_1$ ,  $S_2$ . The correspondence between a WDF and its reference filter is established in the  $\psi$ -domain, i.e., the complex frequency variable  $\psi$  is used instead of the usual variable  $p$ . The simplest and most appropriate choice for  $\psi$  is the bilinear transform of the  $z$ -variable, i.e.,

$$\psi = \frac{z-1}{z+1} = \tanh\left(\frac{pT}{2}\right), \quad z = e^{pT}, \quad T = \frac{1}{F} \quad (2.6)$$

where  $F$  is the sampling frequency.

In both branches of the lattice WDF (see Fig. 2.2(a)),  $S_1(\psi)$  and  $S_2(\psi)$  are allpass functions. Consequently, they may be written (except for possible sign reversals) in the following form [6], [9], [31]:

$$S_1 = -\sigma \frac{g_1(-\psi)}{g_1(\psi)} \quad (2.7a)$$

$$S_2 = \frac{g_2(-\psi)}{g_2(\psi)} \quad (2.7b)$$

where  $\sigma = \pm 1$ ,  $g_1(\psi)$  and  $g_2(\psi)$  are so-called Hurwitz polynomials [10] of degree  $N_1$ , and  $N_2$ .

Further, the transfer functions that are realized by these WDFs are given by

$$s_{11} = s_{22} = \frac{S_1 + S_2}{2} = \frac{h(\psi)}{g(\psi)} \quad (2.8)$$

$$s_{12} = s_{21} = \frac{S_2 - S_1}{2} = \frac{f(\psi)}{g(\psi)} \quad (2.9)$$

where  $h(\psi)$ ,  $f(\psi)$  and  $g(\psi)$  are the so-called canonic polynomials [10], [11].

From (2.7), (2.8), and (2.9) we see that

$$g(\psi) = g_1(\psi) g_2(\psi) \quad (2.10a)$$

$$h(\psi) = \frac{1}{2} \{ g_1(-\psi) g_2(\psi) - \sigma g_1(\psi) g_2(\psi) \} \quad (2.10b)$$

$$f(\psi) = \frac{1}{2} \{ g_1(\psi) g_2(-\psi) + \sigma g_1(\psi) g_2(\psi) \} \quad (2.10c)$$

where  $\sigma = 1$  for  $f$  even and  $\sigma = -1$  for  $f$  odd, and  $g(\psi)$  is a Hurwitz polynomial of degree  $N$ , and  $N = N_1 + N_2$ . In this thesis, we only considered the odd order case, i.e., the case of real coefficients. For even order  $N$ , some modifications have to be made.

Further, the so-called characteristic function is defined by

$$C(\psi) = \frac{s_{11}(\psi)}{s_{12}(\psi)} = \frac{h(\psi)}{f(\psi)} \quad (2.10d)$$

It is also known that the zeros of the polynomials  $g_1(\psi)$  and  $g_2(\psi)$  are alternately distributed in a cyclic manner [6] (see figure 2.4). This property allows the determination of  $g_1(\psi)$  and  $g_2(\psi)$  from  $g(\psi)$ .

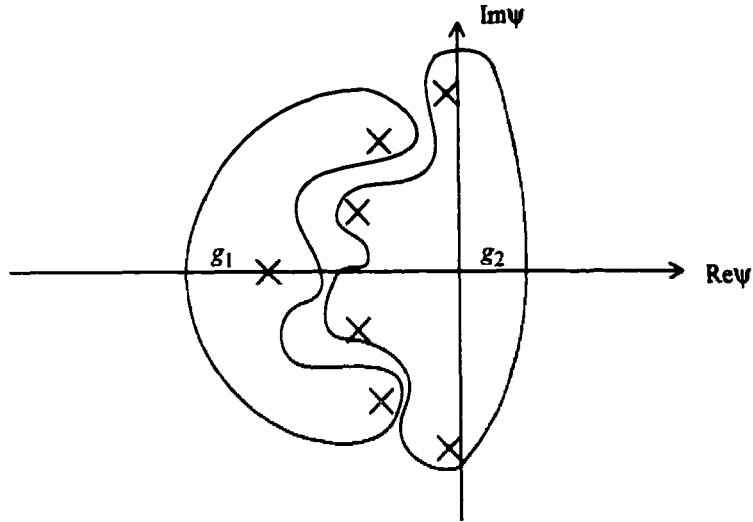


Fig. 2.3 Alternating distribution of the roots of the polynomial  $g_1$  and  $g_2$  (for  $N = 7$ ).

## 2.2 Realization of lattice WDFs

In this section we discuss how to realize allpass functions  $S_1$  and  $S_2$ . An allpass function can be synthesized by several different methods. Here, let us consider the realization as a cascade of elementary sections by means of three-port circulators [12]. We consider the elementary sections of the first- and second-degree.

### 2.2.1 The determination of the multiplier coefficient of a section of degree one

A section of degree one has a reflectance of the form

$$S = \frac{-\psi + B_0}{\psi + B_0} \quad (2.11)$$

It is known (we give a prove below) that using two-port adaptors, the corresponding wave digital realization has an equivalent wave-flow diagram as shown in Figure 2.4, where the coefficient  $\gamma_0$  is given by

$$\gamma_0 = \frac{1 - B_0}{1 + B_0} \quad (2.12)$$

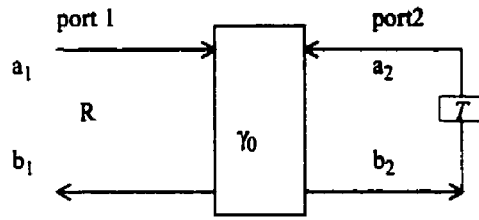


Fig. 2.4 Adaptor representation of an allpass section of degree one.

**Proof:** First rewrite Eq (2.1a) as:

$$a_1 = v_1 + R_1 i_1 \quad (2.13a)$$

$$b_1 = v_1 - R_1 i_1 \quad (2.13b)$$

$$a_2 = v_2 + R_2 i_2 \quad (2.13c)$$

$$b_2 = v_2 - R_2 i_2 \quad (2.13d)$$

Then let us consider the direct connection of two 2-ports, with port resistances  $R_1$  and  $R_2$  shown in Figure 2.5.

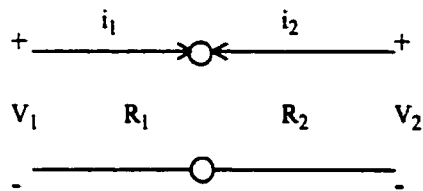


Fig. 2.6 Direct connection of two 2-ports.

Since the two ports are simply connected, we get

$$v_1 = v_2 \quad (2.14a)$$

$$i_1 = -i_2 \quad (2.14b)$$

Then substituting (2.14a) and (2.14b) into (2.13c), we get

$$a_2 = v_1 - R_2 i_1 \quad (2.15)$$

And from (2.13a) and (2.15), we get

$$i_1 = \frac{a_2 - a_1}{R_1 + R_2} \quad (2.16a)$$

$$v_1 = \frac{R_2 a_1 + R_1 a_2}{R_1 + R_2} \quad (2.16b)$$

Substituting (2.16a) and (2.16b) into (2.13b), we get

$$b_1 = a_2 + \gamma_0 (a_2 - a_1) \quad (2.17a)$$

and substituting (2.16a) and (2.16b) into (2.13d), we get

$$b_2 = a_1 + \gamma_0 (a_2 - a_1) \quad (2.17b)$$

where

$$\gamma_0 = \frac{R_1 - R_2}{R_1 + R_2} \quad (2.17c)$$

Also from Figure 2.4, we have

$$a_2 = z^{-1} b_2 \quad (2.18)$$

Substituting (2.18) into (2.17a) and (2.18b)

$$b_1 = (1 + \gamma_0) z^{-1} b_2 - \gamma_0 a_1 \quad (2.19a)$$

$$b_2 = \gamma_0 z^{-1} b_2 + (1 - \gamma_0) a_1 \quad (2.19b)$$

From (2.19b) we get

$$b_2 = \frac{1 - \gamma_0}{1 - \gamma_0 z^{-1}} a_1 \quad (2.20)$$

Substituting (2.20) into (2.19a)

$$S = \frac{b_1}{a_1} = \frac{z^{-1} - \gamma_0}{1 - \gamma_0 z^{-1}} \quad (2.21)$$

Substituting (2.6) into (2.11)

$$S = \frac{-\frac{z-1}{z+1} + B_0}{\frac{z-1}{z+1} + B_0} = \frac{z^{-1} - \frac{1-B_0}{1+B_0}}{1 - \frac{1-B_0}{1+B_0}z^{-1}} \quad (2.22)$$

Comparing (2.21) and (2.22), we get

$$\gamma_0 = \frac{1-B_0}{1+B_0} \quad (2.23)$$

This completes the proof.

### 2.2.2 The determination of the multiplier coefficient of a section of degree two

Each of the  $(N-1)/2$  sections of degree two has (as we shall prove below) a reflectance of the following form:

$$S = \frac{\psi^2 - A_i \psi + B_i}{\psi^2 + A_i \psi + B_i} \quad (2.24)$$

It is known [6] that the corresponding wave digital realization has an equivalent wave-flow diagram as shown in Figure 2.7.

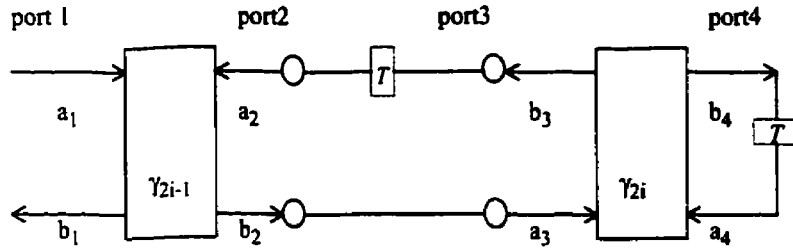


Fig. 2.7 Wave-flow diagrams of the  $i$ th second-degree allpass section.

where the coefficients are given by

$$\gamma_{2i-1} = \frac{A_i - B_i - 1}{A_i + B_i + 1} \quad (2.25a)$$

and

$$\gamma_{2i} = \frac{1 - B_i}{1 + B_i} \quad (2.25b)$$

where  $i = 1, 2, \dots, \frac{N-1}{2}$

**Proof:** First, as in the degree-one case, e.g. from Eq (2.19a,b):

$$b_1 = a_2 + \gamma_{2i-1} (a_2 - a_1) \quad (2.26a)$$

$$b_2 = a_1 + \gamma_{2i-1} (a_2 - a_1) \quad (2.26b)$$

$$b_3 = a_4 + \gamma_{2i} (a_4 - a_3) \quad (2.26c)$$

$$b_4 = a_3 + \gamma_{2i} (a_4 - a_3) \quad (2.26d)$$

Also from Figure 2.7, we have

$$a_2 = z^{-1} b_3 \quad (2.27a)$$

$$a_3 = b_2 \quad (2.27b)$$

$$a_4 = z^{-1} b_4 \quad (2.27c)$$

Then substituting (2.27c) into (2.26d)

$$b_4 = \frac{1 - \gamma_{2i}}{1 - \gamma_{2i} z^{-1}} a_3 \quad (2.28)$$

Substituting (2.27c), (2.28) and (2.27b) into (2.26c)

$$\begin{aligned} b_3 &= (1 + \gamma_{2i}) z^{-1} \left( \frac{1 - \gamma_{2i}}{1 - \gamma_{2i} z^{-1}} \right) a_3 - \gamma_{2i} a_3 \\ &= \left[ \frac{(1 - \gamma_{2i}^2) z^{-1}}{1 - \gamma_{2i} z^{-1}} - \gamma_{2i} \right] a_3 \\ &= \frac{z^{-1} - \gamma_{2i}}{1 - \gamma_{2i} z^{-1}} b_2 \end{aligned} \quad (2.29)$$

Substituting (2.29) into (2.27a)

$$a_2 = z^{-1} \left( \frac{z^{-1} - \gamma_{2i}}{1 - \gamma_{2i} z^{-1}} \right) b_2 \quad (2.30)$$

Substituting (2.30) into (2.26b)

$$a_2 = \frac{(1 - \gamma_{2i-1}) z^{-1} + \gamma_{2i} \gamma_{2i-1} - \gamma_{2i}}{z + \gamma_{2i} \gamma_{2i-1} - \gamma_{2i} - \gamma_{2i-1} z^{-1}} a_1 \quad (2.31)$$

Substituting (2.31) into (2.26a)

$$S = \frac{b_1}{a_1} = \frac{-\gamma_{2i-1} + \gamma_{2i} (\gamma_{2i-1} - 1) z^{-1} + z^{-2}}{1 + \gamma_{2i} (\gamma_{2i-1} - 1) z^{-1} - \gamma_{2i-1} z^{-2}} \quad (2.32)$$

Also, substituting (2.6a) into (2.24)



$$\begin{aligned}
S &= \frac{\left(\frac{z-1}{z+1}\right)^2 - A_i\left(\frac{z-1}{z+1}\right) + B_i}{\left(\frac{z-1}{z+1}\right)^2 + A_i\left(\frac{z-1}{z+1}\right) + B_i} \\
&= \frac{(1 - A_i + B_i)z^2 + (2B_i - 2)z + (1 + A_i + B_i)}{(1 + A_i + B_i)z^2 + (2B_i - 2)z + (1 - A_i + B_i)} \\
&= \frac{-\frac{A_i - B_i - 1}{A_i + B_i + 1} + \frac{2(B_i - 1)}{A_i + B_i + 1}z^{-1} + z^{-2}}{1 + \frac{2(B_i - 1)}{A_i + B_i + 1}z^{-1} - \frac{A_i - B_i - 1}{A_i + B_i + 1}z^{-2}} \tag{2.33}
\end{aligned}$$

Comparing (2.32) and (2.33), we get

$$\gamma_{2i-1} = \frac{A_i - B_i - 1}{A_i + B_i + 1} \tag{2.34}$$

and

$$\gamma_{2i}(\gamma_{2i-1} - 1) = \frac{2(B_i - 1)}{A_i + B_i + 1} \tag{2.35}$$

Substituting (2.34) into (2.35), we get

$$\gamma_{2i} = \frac{1 - B_i}{1 + B_i} \tag{2.36}$$

This completes the proof.

### 2.2.3 Synthesis using cascaded allpass functions

We now discuss direct design methods for lattice WDF realizations of the classical filters using the first- and second-degree allpass sections.

Considering one of the Butterworth, Chebyshev and Cauer (elliptic) reference filters,  $g(\psi)$  can be assumed to have the following product form:

$$g(\psi) = (\psi + B_0) \prod_{i=1}^{\frac{(N-1)}{2}} (\psi^2 + \psi A_i + B_i) \quad (2.37)$$

In the most common cases, i.e., for Butterworth, Chebyshev and Cauer (elliptic) reference filters,  $A_i, B_i$  of (2.37) can be obtained by the formulas given in [6] and [13]. Then from  $g(\psi)$ ,  $g_1(\psi)$  and  $g_2(\psi)$  can be obtained by using the alternating property relating to the distribution of the their zeros. Thus the allpass functions  $S_1$  and  $S_2$  can be written as the following product of sections of degree one and two:

$$S_1(\psi) = \frac{-\psi + B_0}{\psi + B_0} \cdot \frac{\psi^2 - \psi A_2 + B_2}{\psi^2 + \psi A_2 + B_2} \cdot \frac{\psi^2 - \psi A_4 + B_4}{\psi^2 + \psi A_4 + B_4} \cdot \dots \cdot \frac{\psi^2 - \psi A_k + B_k}{\psi^2 + \psi A_k + B_k} \quad (2.38a)$$

$$S_2(\psi) = \frac{\psi^2 - \psi A_1 + B_1}{\psi^2 + \psi A_1 + B_1} \cdot \frac{\psi^2 - \psi A_3 + B_3}{\psi^2 + \psi A_3 + B_3} \cdot \dots \cdot \frac{\psi^2 - \psi A_l + B_l}{\psi^2 + \psi A_l + B_l} \quad (2.38b)$$

where

$$k = \frac{N-1}{2}, \quad l = \frac{N-3}{2}, \quad \text{or } k = \frac{N-3}{2}, \quad l = \frac{N-1}{2}.$$

All adaptor coefficients can be computed by (2.12) and (2.25). Using the cascade synthesis of these elementary sections, realizations of  $S_1$  and  $S_2$  are obtained, which leads to the corresponding block diagram for the filter given in Figure 2.8.

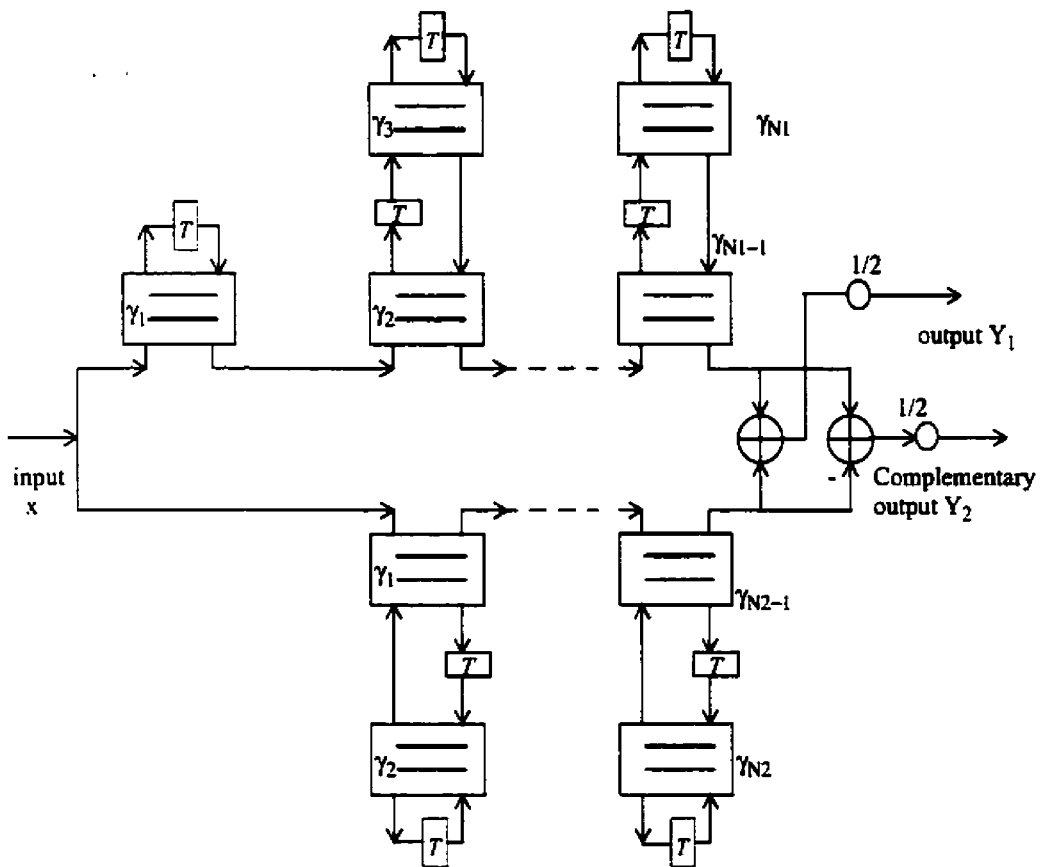


Fig.2.8. Block diagram of the lattice WDF with cascaded allpass sections for order  $N_1$  (as the top structure), or order  $N_2$  (as the bottom structure), the filter order:  $N = N_1 + N_2$ .

The main advantage of this method is that it is direct, simply with easy calculations and it derives the design and implementation of IIR filters at the same time.

**Extensions:** Since general IIR filter (Butterworth, Chebyshev, elliptic) functions are available both in the analog  $\psi$ -domain and digital  $z$ -domain in MATLAB, we only need to decompose those functions into two allpass filters, i.e. realize the filter transfer function (in the  $\psi$ -domain) by using the method shown in sections 2.2.1 and 2.2.2. In order to realize the transfer function in the digital domain, some modifications have to be made:

For a section of degree one, using the bilinear transform  $\psi = \frac{z-1}{z+1}$ , we can rewrite

(2.11) in the form

$$S(z) = \frac{\beta_0 z + 1}{z + \beta_0} \quad (2.39)$$

And (2.21) can be written as

$$S(z) = \frac{-\gamma_0 z + 1}{z - \gamma_0} \quad (2.40)$$

Comparing (2.39) and (2.40), and using (2.23), we get

$$\gamma_0 = -\beta_0 = \frac{1 - B_0}{1 + B_0} \quad (2.41)$$

For a section of degree two, using the bilinear transform  $\psi = \frac{z-1}{z+1}$ , we can rewrite

(2.24) as

$$S(z) = \frac{\beta_i z^2 + \alpha_i z + 1}{z^2 + \alpha_i z + \beta_i} \quad (2.42)$$

And (2.32) can be written as

$$S(z) = \frac{-\gamma_{2i-1} z^2 + \gamma_{2i} (\gamma_{2i-1} - 1) z + 1}{z^2 + \gamma_{2i} (\gamma_{2i-1} - 1) z - \gamma_{2i-1}} \quad (2.43)$$

Comparing (2.42) and (2.43), and using (2.25), we get

$$\gamma_{2i-1} = -\beta_i = \frac{A_i - B_i - 1}{A_i + B_i + 1} \quad (2.44a)$$

$$\gamma_{2i} = \frac{\alpha_i}{-\beta_i - 1} = \frac{1 - B_i}{1 + B_i} \quad (2.44b)$$

And (2.37) can be written as

$$g(z) = (z + \beta_0) \prod_{i=1}^{(N-1)/2} (z^2 + \alpha_i z + \beta_i) \quad (2.45)$$

And (2.38a,b) can be written as

$$S_1(z) = \frac{\beta_0 z + 1}{z + \beta_0} \cdot \frac{\beta_2 z^2 + \alpha_2 z + 1}{z^2 + \alpha_2 z + \beta_2} \cdot \frac{\beta_4 z^2 + \alpha_4 z + 1}{z^2 + \alpha_4 z + \beta_4} \cdot \dots \cdot \frac{\beta_k z^2 + \alpha_k z + 1}{z^2 + \alpha_k z + \beta_k} \quad (2.46a)$$

$$S_2(z) = \frac{\beta_1 z^2 + \alpha_1 z + 1}{z^2 + \alpha_1 z + \beta_1} \cdot \frac{\beta_3 z^2 + \alpha_3 z + 1}{z^2 + \alpha_3 z + \beta_3} \cdot \dots \cdot \frac{\beta_l z^2 + \alpha_l z + 1}{z^2 + \alpha_l z + \beta_l} \quad (2.46b)$$

where

$$k = \frac{N-1}{2}, \quad l = \frac{N-3}{2}, \quad \text{or } k = \frac{N-3}{2}, \quad l = \frac{N-1}{2}.$$

In order to demonstrate the above realization procedure, an example is shown below.

**Example:** Specification:

- $A_p = 1.0$  dB,  $A_s = 42.5$  dB,
- $\omega_p = 20$  rads / sec,  $\omega_s = 30$  rads / sec,
- Sampling freq = 100 rads / sec

1) In  $\psi$  domain: To meet the specification requirement: A 5th order Chebshev lowpass filter transfer function can be gotten in the following closed form by MATLAB:

$$H(\psi) = \frac{f(\psi)}{g(\psi)} = \frac{0.024861}{(\psi + 0.210329)(\psi + 0.064995 \pm j0.719355)(\psi + 0.17016 \pm j0.444586)}$$

Assign the poles to  $g_1(\psi)$ ,  $g_2(\psi)$  by using the alternating property, we get:

$$g_1(\psi) = (\psi + 0.210329)(\psi + 0.064995 + j0.719355)(\psi + 0.064995 - j0.719355)$$

$$g_2(\psi) = (\psi + 0.17016 + j0.444586)(\psi + 0.17016 - j0.444586)$$

$\sigma = 1$  since  $f$  is even. Then using (2.7a,b), we get the corresponding allpass functions:

$$\begin{aligned} S_1(\psi) &= \frac{-\sigma g_1(-\psi)}{g_1(\psi)} = \frac{-(-\psi + 0.210329)(-\psi + 0.064995 \pm j0.719355)}{(\psi + 0.210329)(\psi + 0.064995 \pm j0.719355)} \\ &= \frac{-(-\psi + 0.210329)(\psi^2 - 0.12999\psi + 0.521696)}{(\psi + 0.210329)(\psi^2 + 0.12999\psi + 0.521696)} \end{aligned}$$

$$\begin{aligned} S_2(\psi) &= \frac{g_2(-\psi)}{g_2(\psi)} = \frac{(-\psi + 0.17016 + j0.444586)(-\psi + 0.17016 - j0.444586)}{(\psi + 0.17016 + j0.444586)(\psi + 0.17016 - j0.444586)} \\ &= \frac{\psi^2 - 0.34032\psi + 0.226611}{\psi^2 + 0.34032\psi + 0.226611} \end{aligned}$$

Realize  $S_1(\psi)$ ,  $S_2(\psi)$  by using (2.12, 2.25), we get

$$\gamma_1 = 0.652443, \gamma_2 = -0.842597, \gamma_3 = 0.314323,$$

$$\gamma_4 = -0.565622, \gamma_5 = 0.630509.$$

2) In the digital domain: To meet the same specification requirement: The corresponding 5th order Chebyshev lowpass filter has the poles:

$$p_0 = 0.65243, p_{1,2} = 0.493569 \pm j0.567461, p_{3,4} = 0.289585 \pm j0.871055.$$

Assign the poles to  $g_1(z)$  and  $g_2(z)$  by using the pole interlace property:

$$S_1(z) = \frac{-(-0.652443z + 1)}{(z - 0.652443)} \cdot \frac{(0.842596z^2 - 0.57917z + 1)}{(z^2 - 0.57917z + 0.842596)}$$

$$S_2(z) = \frac{(0.565622z^2 - 0.987138z + 1)}{(z^2 - 0.987138z + 0.565622)}$$

Realize  $S_1(z)$ ,  $S_2(z)$  by using (2.41), (2.44a,b):

$$\gamma_1 = 0.652443, \gamma_2 = -0.842596, \gamma_3 = 0.314323,$$

$$\gamma_4 = -0.565622, \gamma_5 = 0.630509.$$

Note: They are same as those obtained above using the polynomials in the  $\psi$  domain.

Finally, we implement the filter by using the structure shown in Fig. 2.9.

The frequency responses are presented in Fig 2.10 which shows that the specifications are satisfied.

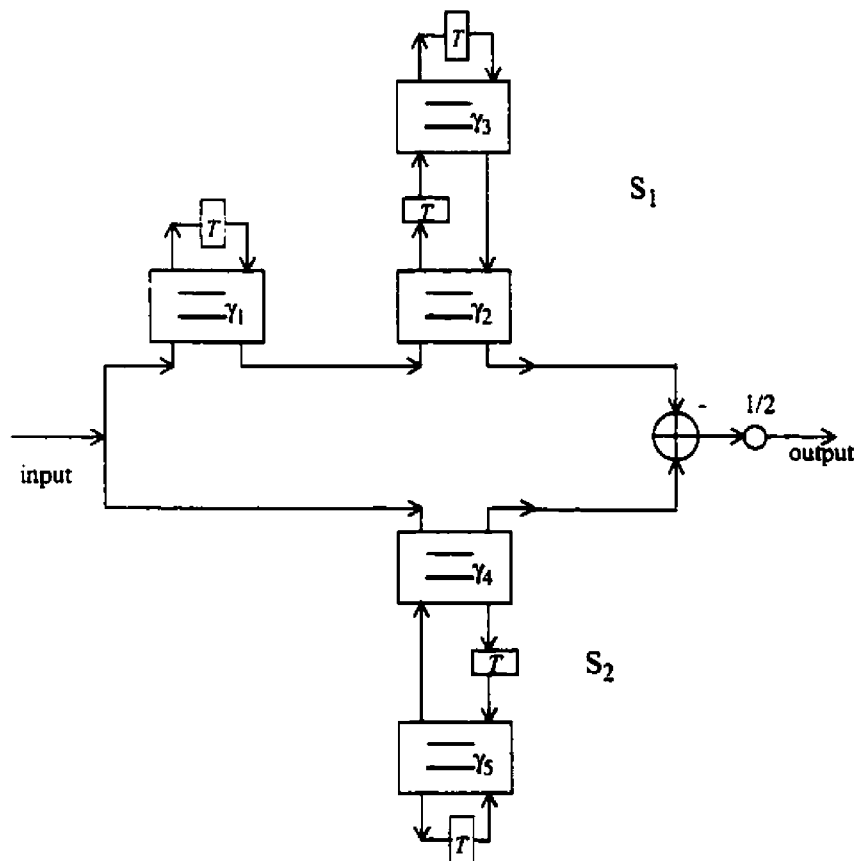


Fig. 2.9 Realization structure of the example.

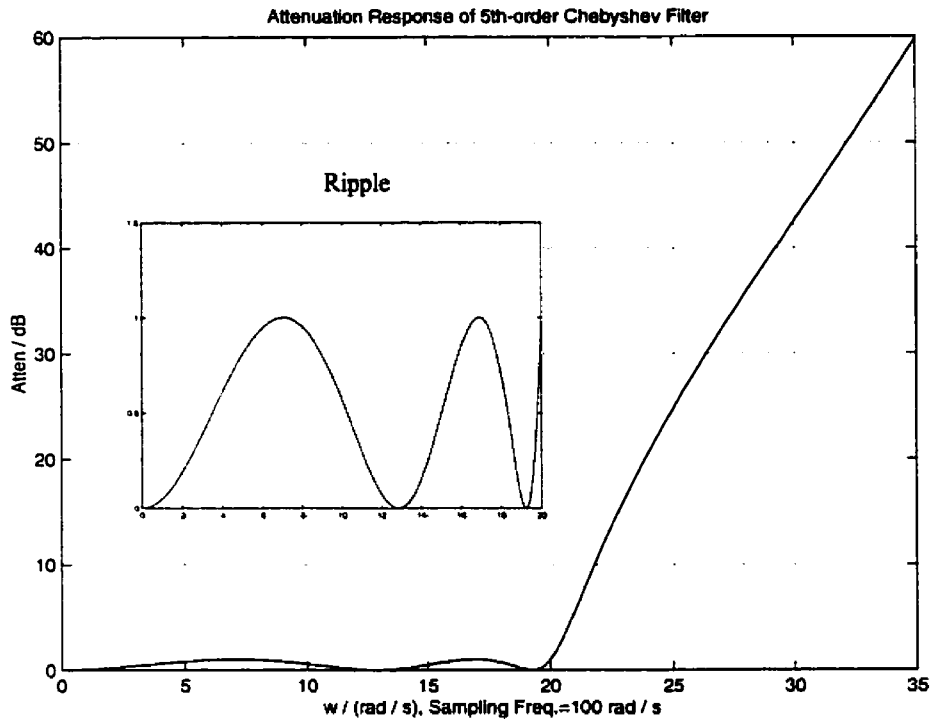


Fig. 2.10

## 2.3 Bireciprocal lattice WDF design

IIR bireciprocal filters are used in many communication systems in the case of interpolation or decimation with a factor of two. The sampling rate alteration can be implemented very economically in a bireciprocal lattice WDF which leads to enormous savings in hardware. In this section, we will modify the standard elliptic filter design and realization, then an example which demonstrate this procedure is given.

### 2.3.1 The definition of bireciprocal filters [14]

A bireciprocal lattice WDF is a special case of a lattice WDF, it is formed by the characteristic function [14]. That is, if the characteristic function



$$K(\psi) = \frac{h(\psi)}{f(\psi)} \quad (2.47)$$

satisfies

$$K\left(\frac{1}{\psi}\right) = \frac{1}{K(\psi)} \quad (2.48)$$

then the characteristic function is called a bireciprocal or a mirror-image function, and the

corresponding filter  $H(\psi) = \frac{f(\psi)}{g(\psi)}$  is called a bireciprocal filter. Based on the definition

of a bireciprocal filter defined by (2.47), the following properties [14] of  $f(\psi)$ ,  $g(\psi)$

and  $h(\psi)$  hold

$$h(\psi) = \pm \psi^n f\left(\frac{1}{\psi}\right), \quad f(\psi) = \pm \psi^n h\left(\frac{1}{\psi}\right) \quad (2.49a,b)$$

$$g(\psi) = \pm \psi^n g\left(\frac{1}{\psi}\right) \quad (2.50)$$

where  $n$  is the degree of  $g(\psi)$  and the polynomials are real.

According to the above definition, the passband and stopband attenuation of a bireciprocal filter are related by

$$A_p = -10 \log_{10} \left( 1 - 10^{(-A_s/10)} \right) \quad (2.51)$$

and the frequency relation between  $\omega_p$  and  $\omega_s$  for a bireciprocal filter is

$$\omega_s T + \omega_p T = \pi \quad (2.52a)$$

or (in the  $\psi$  domain)

$$\phi_s = 1/\phi_p \quad (2.52b)$$

where  $\varphi_s = \tan\left(\frac{\omega_s}{2F}\right)$ ,  $\varphi_p = \tan\left(\frac{\omega_p}{2F}\right)$ ,  $F$  is the sampling frequency.

### 2.3.2 The design method of bireciprocal elliptic filters

Since the bireciprocal elliptic filter is a special case of the elliptic filter, it is possible to modify the standard elliptic filter algorithm such that the (2.51), (2.52) are exactly satisfied.

We organize the design procedure as follows:

- Specify  $A_s$  and  $\omega_s$ , then calculate  $A_p$  and  $\omega_c$  by using the (2.51), (2.52).
- Use a program (e.g. MATLAB) for cauer filter design with the above specifications to find the transfer function.
- Use the transfer function to find  $f, g, h$  (described in section 2.2), and to compute the adaptor coefficients.

### 2.3.3 The realization structure of bireciprocal elliptic filters

Once the transfer function is obtained, the realization method described in section 2.2 still applies. We can rewrite (2.37) as

$$g(\psi) = (\psi + 1) \prod_{i=1}^{\frac{N-1}{2}} (\psi^2 + \psi A_i + 1) \quad (2.53)$$

and (3.38) can be written as

$$S_1(\psi) = \frac{-\psi + 1}{\psi + 1} \cdot \frac{\psi^2 - \psi A_2 + 1}{\psi^2 + \psi A_2 + 1} \cdot \dots \cdot \frac{\psi^2 - \psi A_k + 1}{\psi^2 + \psi A_k + 1} \quad (2.54a)$$

$$S_2(\psi) = \frac{\psi^2 - \psi A_1 + 1}{\psi^2 + \psi A_1 + 1} \cdot \frac{\psi^2 - \psi A_3 + 1}{\psi^2 + \psi A_3 + 1} \cdot \dots \cdot \frac{\psi^2 - \psi A_l + 1}{\psi^2 + \psi A_l + 1} \quad (2.54b)$$

where

$$k = \frac{N-1}{2}, \quad l = \frac{N-3}{2}, \quad \text{or } k = \frac{N-3}{2}, \quad l = \frac{N-1}{2}.$$

Apply the realization method in section 2.2, it is easy to show:

For a section of degree one

$$\gamma_0 = 0$$

then Fig. 2.4 can be simplified to the bireciprocal wave flow diagram of degree one:

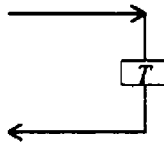


Fig. 2.11(a) Wave flow diagram for the degree one.

For a section of degree two

$$\gamma_{2i} = 0$$

$$\gamma_{2i-1} = \frac{A_i - 2}{A_i + 2}$$

then Fig. 2.7 can be simplified to a bireciprocal wave flow diagram of degree two.

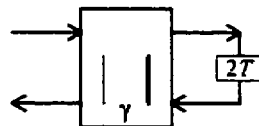


Fig. 2.11(b) Wave flow diagram for the degree two.

Furthermore, Fig. 2.8 can be simplified to the realization structure for a bireciprocal filter as in Fig. 2.11c.

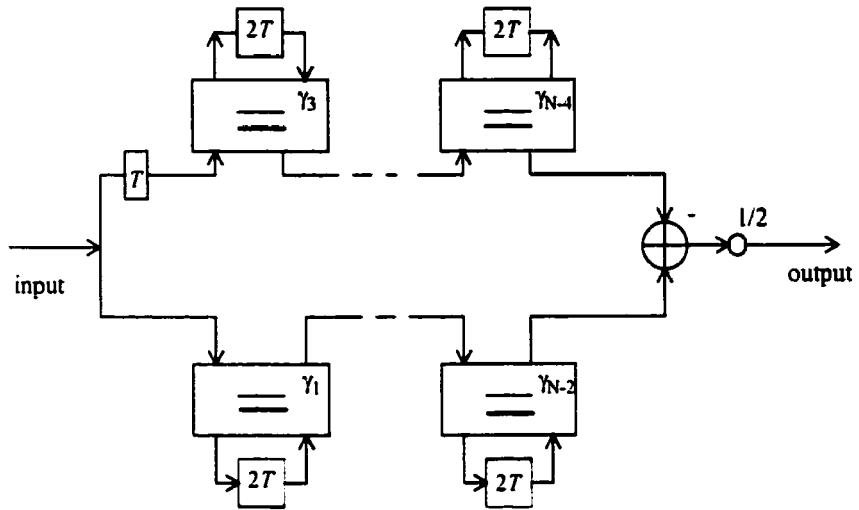


Fig. 2.11(c) Realization structure of birciprocal filter of order  $N$ .

To demonstrate the above design procedure, an example is given below.

**Example: Specification:**

- $A_p = 0.1 \text{ dB}$ ,  $A_s = 68 \text{ dB}$ ,
- $f_p = 8 \text{ kHz}$ ,  $f_s = 16 \text{ kHz}$ ,
- Sampling freq =  $48 \text{ kHz}$ .

The coefficients of the three 2-port adaptors can be obtained by following the above design procedure as

$$\gamma_1 = -0.09213253378103, \gamma_2 = -0.34345544384394, \gamma_3 = -0.73104262493127$$

After 11 bit quantization, the three parameters become

$$\gamma_1 = -189/2048, \gamma_2 = -352/1024, \gamma_3 = -749/1024.$$

The realization structure for the example is shown in Fig. 2.12.

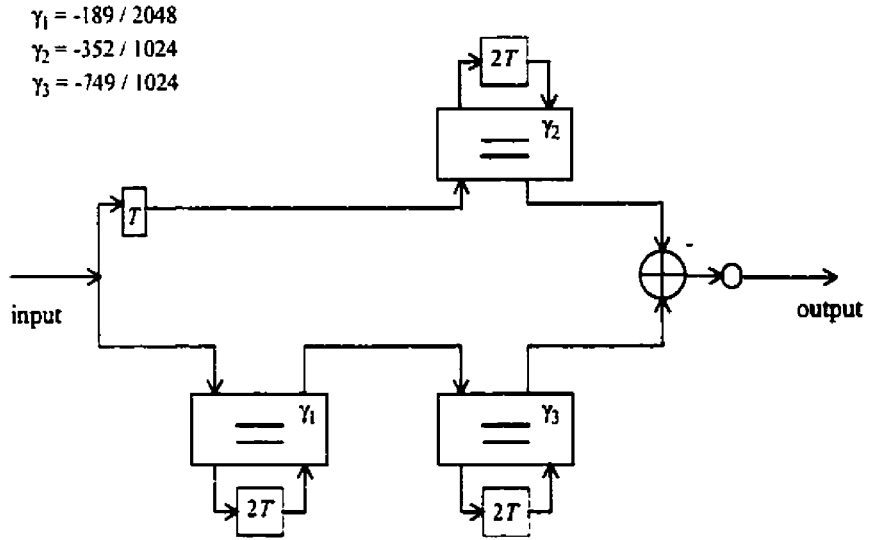


Fig. 2.12 Realization structure of the example.

The frequency responses are presented in Fig. 2.13a,b which shows that the specifications are satisfied.

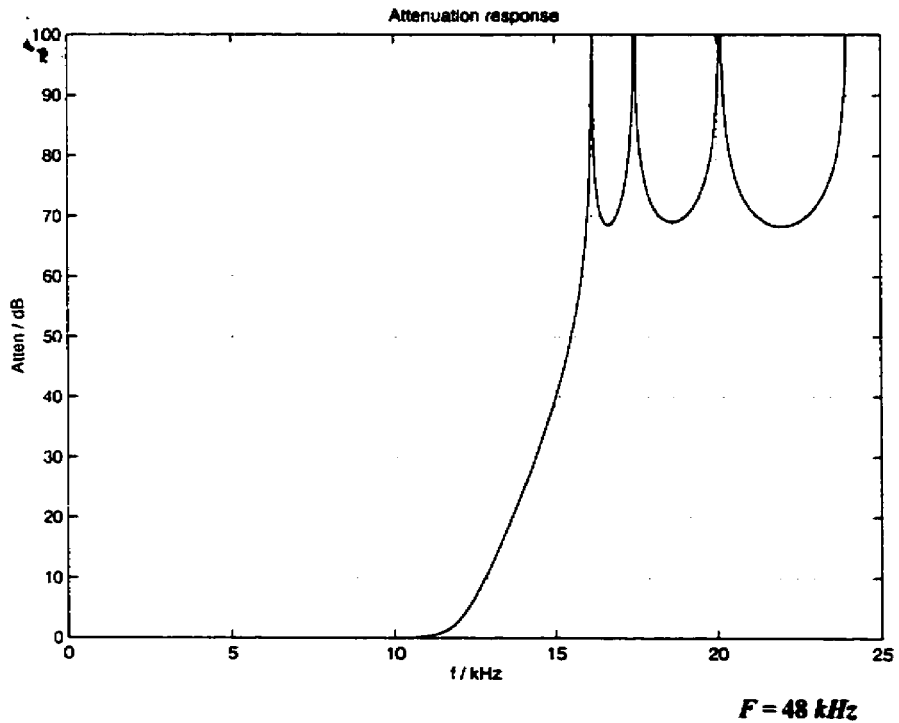


Fig. 2.13(a) Attenuation response of the example.

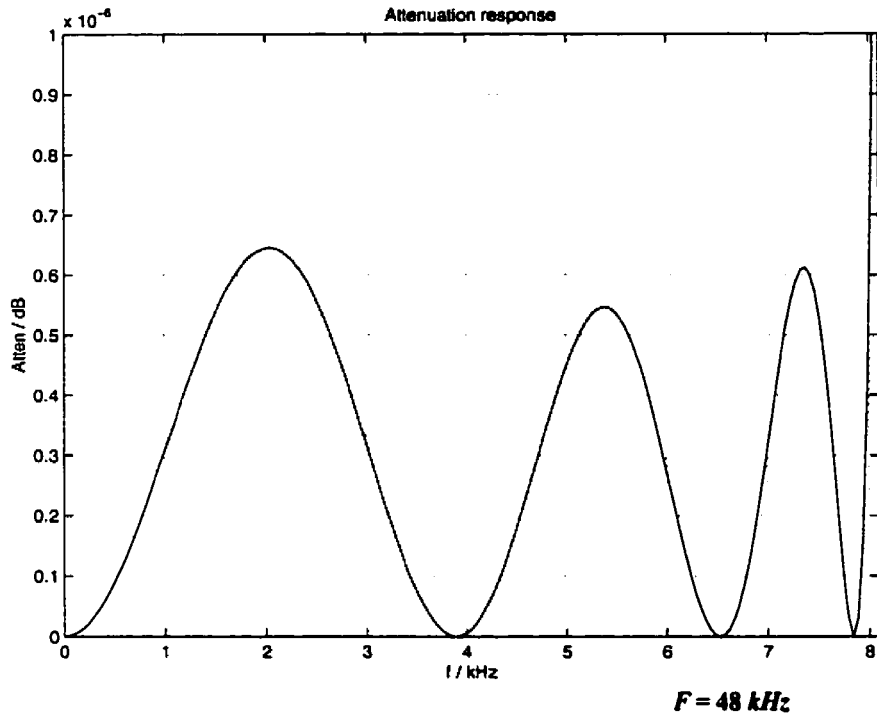


Fig. 2.13(b) Ripple response of the example.

# Chapter 3

## *IIR multiple notch filter design*

In this section, an IIR multiple notch filter design based on the phase of an allpass filter approximation will be described [15].

### 3.1 A multiple notch filter design method

Generally, the input of the notch filter has the following form

$$x(n) = s(n) + \sum_{k=1}^M A_k \sin(n\omega_{Nk} + \phi_k) = s(n) + d(n) \quad (3.1)$$

where  $s(n)$  is a desired signal,  $d(n)$  is a sum of sinusoidal interference signals with frequencies  $\omega_{Nk} \in (0, \pi)$  for  $k = 1, \dots, M$ ,  $M$  is the number of sinusoidal interference signals.

In order to extract  $s(n)$  from the corrupted signal  $x(n)$  without distortion, the specification of an ideal notch filter is given by

$$H(e^{j\omega}) = \begin{cases} 0 & \omega = \omega_{Nk}, k = 1, \dots, M \\ 1 & \text{otherwise} \end{cases} \quad (3.2)$$

Further, the IIR notch filter  $H(z)$  studied here has the following form in the digital domain:

$$H(z) = \frac{1}{2}(1 + A(z)) \quad (3.3)$$

where  $A(z)$  is an allpass function.

### 3.1.1 Specification transformation

In the following, we will use the relation (3.3) to transform the specification of a multiple notch filter into that of an allpass filter. As a result, the notch filter design problem becomes an allpass filter design problem.

The transfer function of a  $2M$  order allpass filter  $A(z)$  is defined by

$$A(z) = \frac{a_{2M} + \dots + a_1 z^{-2M+1} + z^{-2M}}{1 + a_1 z^{-1} + \dots + a_{2M} z^{-2M}} \quad (3.4)$$

Since for  $z = e^{j\omega}$  the magnitude response of the allpass  $A(z)$  is equal to unity for all frequencies, the frequency response can be written as

$$A(e^{j\omega}) = e^{j\theta_A(\omega)} \quad (3.5)$$

where  $\theta_A(\omega)$  is the allpass filter phase response. From (3.4) and (3.5), we have

$$A(e^{j\omega}) = \frac{\sum_{k=0}^{2M} a_k e^{-j\omega(2M-k)}}{\sum_{k=0}^{2M} a_k e^{-j\omega k}} \quad (3.6)$$

Now let  $\theta_d$  and  $\theta_n$  denote the angle of the denominator and the numerator of (3.6),

respectively, then

$$\theta_d(\omega) = \angle \sum_{k=0}^{2M} a_k e^{-j\omega k}$$



$$\begin{aligned}
&= \angle \sum_{k=0}^{2M} a_k (\cos \omega k - j \sin \omega k) \\
&= -\tan^{-1} \left( \frac{\sum_{k=0}^{2M} a_k \sin(\omega k)}{\sum_{k=0}^{2M} a_k \cos(\omega k)} \right) \\
&= -\tan^{-1} \left( \frac{\sum_{k=1}^{2M} a_k \sin(\omega k)}{1 + \sum_{k=1}^{2M} a_k \cos(\omega k)} \right) \tag{3.7a}
\end{aligned}$$

and

$$\begin{aligned}
\theta_n(\omega) &= \angle \sum_{k=0}^{2M} a_k e^{-j\omega(2M-k)} \\
&= \angle \sum_{k=0}^{2M} a_k e^{-j2M\omega} e^{j\omega k} \\
&= \angle e^{-j2M\omega} \sum_{k=0}^{2M} a_k e^{j\omega k} \\
&= -2M\omega - \theta_d(\omega) \tag{3.7b}
\end{aligned}$$

From (3.6) and (3.7b), we get

$$\theta_A(\omega) = \angle A(e^{j\omega}) = \theta_n(\omega) - \theta_d(\omega) = -2M\omega - 2\theta_d(\omega) \tag{3.8}$$

And from (3.7a) and (3.8), we get

$$\theta_A(\omega) = -2M\omega + 2 \tan^{-1} \left( \frac{\sum_{k=1}^{2M} a_k \sin(\omega k)}{1 + \sum_{k=1}^{2M} a_k \cos(\omega k)} \right) \quad (3.9)$$

From (3.9), the  $\theta_A(\omega)$  of a stable allpass filter is zero when  $\omega = 0$ ,  $-2M\pi$  when  $\omega = \pi$ , and is required to decrease monotonically with increasing frequency [16].

**Proof:** First-order case. Since the poles and zeros of a real allpass function occur in reciprocal conjugate pairs, we can write a first order allpass transfer function as

$$H(z) = \frac{a^* + z^{-1}}{1 + az^{-1}}, \text{ where } a^* \text{ is the conjugate of } a. \text{ Now let } r \text{ and } \theta \text{ represent the radius}$$

and angle of  $a$ , so that  $a = re^{j\theta}$ . Then

$$\begin{aligned} H(e^{j\omega}) &= \frac{re^{-j\theta} + e^{-j\omega}}{1 + re^{j\theta} e^{-j\omega}} \\ &= e^{-j\omega} \frac{1 + re^{j(\omega-\theta)}}{1 + re^{-j(\omega-\theta)}} \end{aligned} \quad (3.10)$$

The phase response  $\phi(\omega)$  can be obtained immediately

$$\phi(\omega) = -\omega + 2 \tan^{-1} \frac{r \sin(\omega - \theta)}{1 + r \cos(\omega - \theta)} \quad (3.11)$$

Differentiating with respect to  $\omega$  we arrive at

$$\frac{d\phi(\omega)}{d\omega} = \frac{-(1-r^2)}{(1-r)^2 + 2r(1 + \cos(\omega - \theta))} \quad (3.12)$$

If the pole is inside the unit circle, e.g.  $0 \leq r < 1$ , we have  $\frac{d\phi(\omega)}{d\omega} < 0$ , that is,  $\phi(\omega)$  is

monotonically decreasing.

Since an  $N$ -th order stable allpass function is a product of  $N$  first-order stable allpass functions, its (unwrapped) phase response is the sum of the  $N$  individual phase responses, and is thus monotone. This completes the proof.

Moreover we can also write the frequency response of a notch filter  $H(z)$  as follows:

$$\begin{aligned} H(e^{j\omega}) &= \frac{1}{2} \left( 1 + e^{j\theta_A(\omega)} \right) \\ &= \frac{1}{2} e^{j\frac{\theta_A(\omega)}{2}} \left( e^{-j\frac{\theta_A(\omega)}{2}} + e^{j\frac{\theta_A(\omega)}{2}} \right) = e^{j\frac{\theta_A(\omega)}{2}} \cos\left(\frac{\theta_A(\omega)}{2}\right) \end{aligned} \quad (3.13)$$

From (3.13), we can show that the magnitude response of a notch filter is related to the phase of allpass filter as follows:

$$\left| H(e^{j\omega}) \right| = \left| \cos\left(\frac{\theta_A(\omega)}{2}\right) \right| \quad (3.14)$$

And from (3.9) and the monotone phase property of an allpass filter, it is clear that the phase  $\theta_A(\omega)$  goes from 0 to  $-2M\pi$ , when  $\omega$  goes from 0 to  $\pi$  radians. Based on this property and (3.14), we have the following observations:

(1) There exist  $M$  frequency points  $\omega_1 < \omega_2 < \dots < \omega_M$  such that

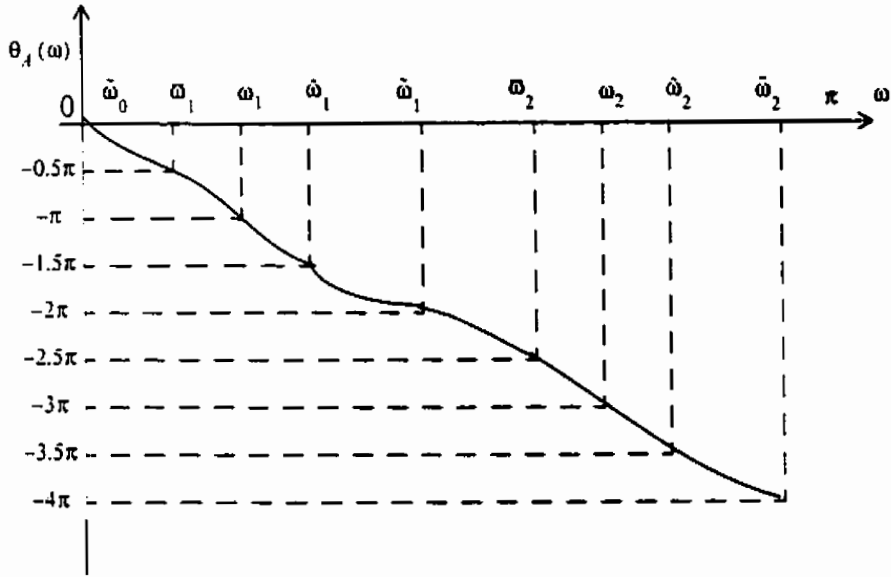
$$\theta_A(\omega_n) = -(2n-1)\pi, \text{ that is } H(e^{j\omega_n}) = 0 \text{ for } n = 1, \dots, M.$$

(2) There exist  $M$  frequency points  $\varpi_1 < \varpi_2 < \dots < \varpi_M$  such that

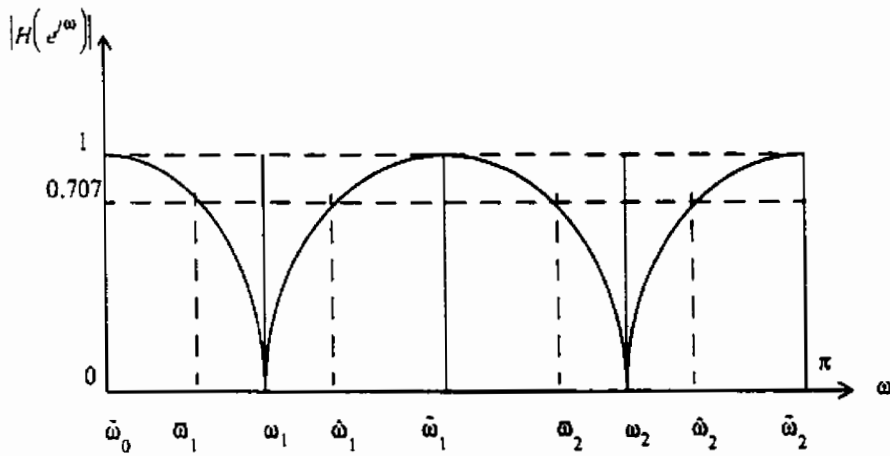
$$\theta_A(\varpi_n) = -(2n-1)\pi + \frac{\pi}{2}, \text{ that is, } \left| H(e^{j\varpi_n}) \right| = \left| \frac{1}{2}(1-j) \right| = \frac{1}{\sqrt{2}} \text{ for } n = 1, \dots, M.$$

(3) There exist  $M$  frequency points  $\hat{\omega}_1 < \hat{\omega}_2 < \dots < \hat{\omega}_M$  such that

$$\theta_A(\hat{\omega}_n) = -(2n-1)\pi - \frac{\pi}{2}, \text{ that is, } \left| H(e^{j\hat{\omega}_n}) \right| = \left| \frac{1}{2}(1+j) \right| = \frac{1}{\sqrt{2}} \text{ for } n=1, \dots, M.$$



(a)



(b)

Fig. 3.1. (a) phase response of allpass filter. (b) magnitude response of notch filter.

(4) There exist  $M+1$  frequency points  $0 = \tilde{\omega}_0 < \tilde{\omega}_1 < \dots < \tilde{\omega}_M = \pi$  such that

$$\theta_A(\tilde{\omega}_n) = -2n\pi, \text{ that is, } H(\tilde{\omega}_n) = 1 \text{ for } n = 0, 1, \dots, M.$$

Now let  $H(z)$  be a fourth order notch filter, i.e.,  $M = 2$ , a graphic interpretation of these four observations is shown in Fig 3.1. It is obvious that the four statements are valid.

Moreover from (3.14), we can see that the maximum gain of the magnitude response of a notch filter is unity. Based on the above observation, if we want to design a notch filter  $H(z)$  which satisfies the specification shown in Fig 3.2, we need to make the following

assignments of the phase  $\theta_A(\omega)$  of the allpass filter  $A(z)$  :

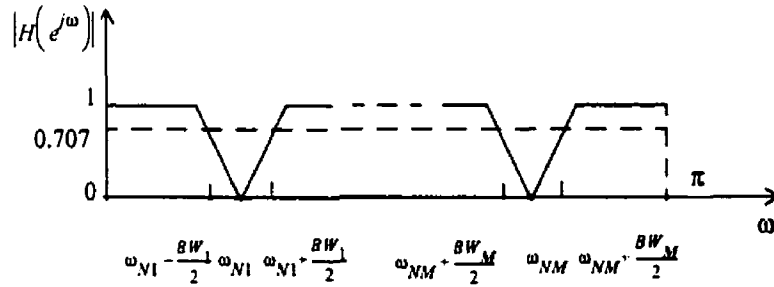


Fig. 3.2. The prescribed specification of the real coefficient notch filter.

- 1)  $\theta_A(\omega_{Nn}) = -(2n - 1)\pi$ .
- 2)  $\theta_A\left(\omega_{Nn} - \frac{BW_n}{2}\right) = -(2n - 1)\pi + \frac{\pi}{2}$ .
- 3)  $\theta_A\left(\omega_{Nn} + \frac{BW_n}{2}\right) = -(2n - 1)\pi - \frac{\pi}{2}$ .

where  $n = 1, \dots, M$  and the notch frequency points  $\omega_{Nn}$  satisfy  $\omega_{N1} < \dots < \omega_{NM}$ . Moreover, if  $BW_n$  is very small,  $\theta_A(\omega_{Nn}) = -(2n - 1)\pi$  and

$\theta_A\left(\omega_{Nn} - \frac{BW_n}{2}\right) = -(2n-1)\pi + \frac{\pi}{2}$ , then to a first-order approximation it can be shown

that

$$\theta_A\left(\omega_{Nn} + \frac{BW_n}{2}\right) \approx -(2n-1)\pi - \frac{\pi}{2} \quad (3.15)$$

Thus, assignments (1) and (2) imply assignment (3) if the rejection bandwidth  $BW_n$  is

very small. The three assignments can be reduced to two assignments as follows:

$$(1) \theta_A(\omega_{Nn}) = -(2n-1)\pi.$$

$$(2) \theta_A\left(\omega_{Nn} - \frac{BW_n}{2}\right) = -(2n-1)\pi + \frac{\pi}{2}.$$

where  $n = 1, \dots, M$  and the notch frequency points  $\omega_{Nn}$  satisfy  $\omega_{N1} < \dots < \omega_{NM}$ . After

suitable arrangement, these two assignments are equivalent to the following condition in

$2M$  frequency sampling points. With the frequency points

$$\omega_i = \omega_N \left\lfloor \frac{i+1}{2} \right\rfloor - \frac{1}{2} \left( 1 - (-1)^{\text{mod}(i,2)} \right) \frac{BW \left\lfloor \frac{i+1}{2} \right\rfloor}{2} \quad (3.16)$$

the desired phase response is specified by

$$\theta_A(\omega_i) = -\left( 2 \left\lfloor \frac{i+1}{2} \right\rfloor - 1 \right) \pi + \frac{1}{2} \left( 1 - (-1)^{\text{mod}(i,2)} \right) \frac{\pi}{2} \quad (3.17)$$

where  $i = 1, \dots, 2M$ ,  $\lfloor x \rfloor$  denotes the largest integer which is smaller than or equal to  $x$ , and

$\text{mod}(x,2)$  denotes the remainder when  $x$  is divided by 2.

So far, the specification of the notch filter in Fig 3.2 has been transformed into the specification of an allpass filter. Thus, we only need to design an allpass filter  $A(z)$  which sat-

isfies these  $2M$  requirements in (3.17), then  $\frac{1}{2}(1 + A(z))$  is the desired filter.

### 3.1.2 The structure of the lattice realization

In the following, we first develop an approach to determine the allpass filter coefficients, then, an efficient lattice-form realization is presented.

#### 3.1.2.1 The determination of the allpass filter coefficients

First, from (3.9) and (3.17), we can see that the phase response  $\theta_A(\omega)$  is given at  $2M$  points  $\omega_i, i = 1, \dots, 2M$ . Thus, we can let

$$\frac{\sum_{k=1}^{2M} a_k \sin(k\omega_i)}{1 + \sum_{k=1}^{2M} a_k \cos(k\omega_i)} = \tan(\beta_i), \quad i = 1, 2, \dots, 2M \quad (3.18)$$

where  $\beta_i = \frac{1}{2}(\theta_A(\omega_i) + 2M\omega_i)$ . This expression can be rewritten as

$$\sum_{k=1}^{2M} [\sin(k\omega_i) - \tan(\beta_i) \cos(k\omega_i)] a_k = \tan(\beta_i), \quad i = 1, \dots, 2M \quad (3.19)$$

Note, equation (3.19) is a linear equation in the filter coefficients  $a_k$ , and it can be expressed in the following matrix form:

$$Qa = P \quad (3.20)$$

where the two vectors are

$$a = [a_1 \ a_2 \ \dots \ a_{2M}]^t \quad (3.21a)$$

$$P = [\tan(\beta_1) \ \tan(\beta_2) \ \dots \ \tan(\beta_{2M})]^t \quad (3.21b)$$

and the elements of the matrix  $Q$  are given by

$$q_{ik} = \sin(k\omega_i) - \tan(\beta_i) \cos(k\omega_i), \quad i = 1, \dots, 2M. \quad k = 1, \dots, 2M. \quad (3.22)$$

Solving the linear equation (3.20), the desired solution is given by

$$a = Q^{-1}P \quad (3.23)$$

Thus, the allpass filter coefficients are obtained.

### 3.1.2.2 Lattice realization structure

Since  $H(z) = \frac{1}{2}(1 + A(z))$ , the notch filter can be implemented using the structure

shown in Figure 3.3.

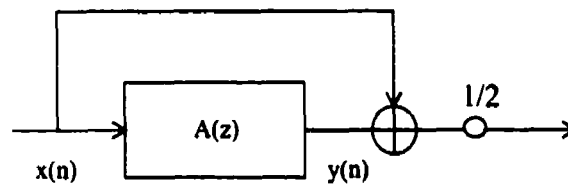


Fig 3.3 The realization of notch filter

Thus, the notch filter realization is equivalent to the realization of an allpass filter. Due to the mirror-image symmetry relation between the numerator and denominator polynomials of an allpass filter,  $A(z)$  can be realized by the computationally efficient lattice structure shown in Figure 3.4.



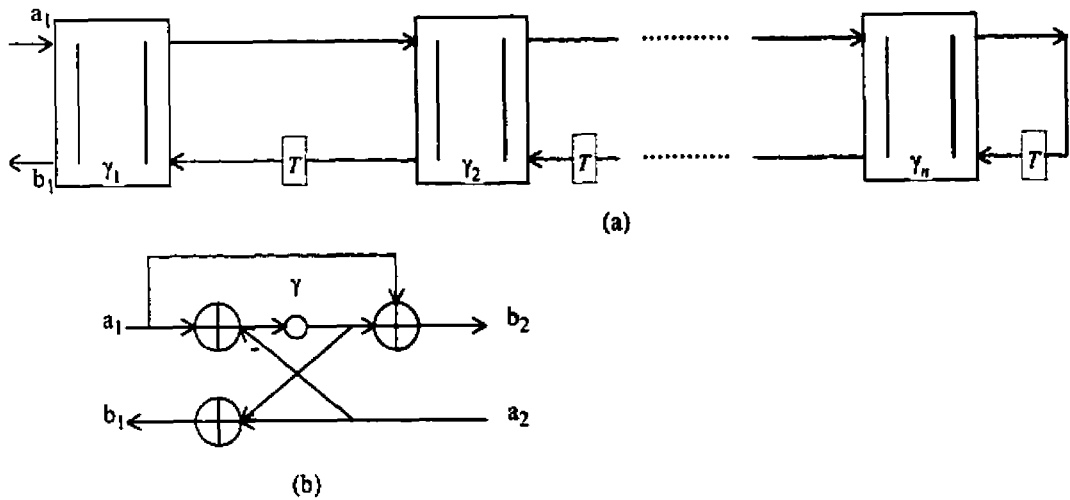


Fig. 3.4 (a) Lattice realization structure of real coefficient allpass filter.

(b) Details of the building blocks.

When the filter coefficients of the direct-form allpass filter are obtained in terms of the above procedure, the lattice coefficients (e.g. the adaptor parameters)  $\gamma$  can be obtained by using the transform method [17] described below. We can use the transfer function of the allpass filter to find the adaptor coefficients  $\gamma$ s. The numerator and denominator of the allpass filter transfer function were used to find the value of the resultant of the division of the two polynomials at  $z^{-1}$  equal to zero.

i.e.

$$A(z) = \frac{h(z^{-1})}{g(z^{-1})} \quad (3.24)$$

where  $A(z)$  is the transfer function of the allpass filter,  $h$  and  $g$  are the numerator and the denominator of the transfer function respectively. Let  $h_1 = h$  and  $g_1 = g$ , then

$$\gamma_1 = \frac{h_1(0)}{g_1(0)} \quad (3.25)$$

this gives the value of  $\gamma_1$ . Then the numerator of a new transfer function is found using the equation below:

$$h_2(z) = \frac{h_1(z^{-1}) - \gamma_1 g_1(z^{-1})}{z^{-1}} \quad (3.26)$$

and the denominator is found using the following equation:

$$g_2(z) = g_1(z^{-1}) - \gamma_1 g_1(z^{-1}) \quad (3.27)$$

now, using  $h_2$  and  $g_2$ , the value of  $\gamma_2$  can be found as  $\gamma_2 = \frac{h_2(0)}{g_2(0)}$ . The process is con-

tinued by increasing the indices by 1 and repeating the process until the final numerator and denominator are constants.

## 3.2 The design procedure and an example

In this section, we first summarize the above design procedure, then, an example which demonstrates this procedure will be given.

### 3.2.1 Summary of design procedure

We summarize the entire design procedure of the IIR multiple notch filter as follows:

1) prescribe notch frequencies  $\omega_{N1} < \omega_{N2} < \dots < \omega_{NM}$  and 3 dB rejection bandwidth

$$BW_1, BW_2, \dots, BW_M;$$

2) using (3.16) and (3.17) compute  $\omega_i$  and  $\theta_A(\omega_i)$ ,  $i = 1, 2, \dots, 2M$ ;

- 3) using (3.21) and (3.22) calculate Q and P. Then, find the allpass filter coefficients  $a_i$ ,  $i = 1, 2, \dots, 2M$  by using (3.23);
- 4) the notch filter is obtained as

$$H(z) = \frac{1}{2} \left( 1 + \frac{a_{2M}z^{2M} + \dots + a_1z^{-2M+1} + z^{-2M}}{1 + a_1z^{-1} + \dots + a_{2M}z^{-2M}} \right) \quad (3.28)$$

- 5) using (3.24) - (3.26) find adaptor coefficients  $\gamma_i$ ,  $i = 1, 2, \dots, 2M$ .

Due to the mirror-image symmetry relation between the numerator and denominator polynomials of an allpass filter, the  $A(z)$  can be realized by computationally efficient lattice structure shown in Fig 3.4. This structure has the minimum number of multipliers and delays. When the filter coefficients  $a_i$  of the allpass filter are obtained in terms of the proposed design procedure, the lattice coefficients  $\gamma_i$ ,  $i = 1, \dots, 2M$  can be obtained by using the method described above. Moreover, the frequency response of the notch filter is very insensitive with respect to the coefficients  $\gamma_i$ ,  $i = 1, \dots, 2M$ , and the notch filter is stable if  $|\gamma_i| < 1$ ,  $i = 1, \dots, 2M$ .

### 3.2.2 The design example

In this section, a design example is presented.

Example: the specification of a sixth-order notch filter is

$$\omega_{1N} = 0.1\pi \quad BW_1 = 0.01\pi$$

$$\omega_{2N} = 0.4\pi \quad BW_2 = 0.01\pi$$

$$\omega_{3N} = 0.7\pi \quad BW_3 = 0.02\pi$$

Using the above design method, we obtain the filter coefficients of a sixth-order allpass fil-

ter as follows:

$$a_1 = -1.3422 \quad a_4 = 1.0897$$

$$a_2 = 1.1918 \quad a_5 = -1.1868$$

$$a_3 = -1.2294 \quad a_6 = 0.8809$$

and the lattice filter coefficients  $\gamma_i$  as follows:

$$\gamma_1 = -0.75845 \quad \gamma_4 = 0.1520$$

$$\gamma_2 = 0.4130 \quad \gamma_5 = -0.01969$$

$$\gamma_3 = -0.4428 \quad \gamma_6 = 0.8809$$

The magnitude and phase response of the notch filter are shown in Figure 3.5. From the results, we see that the specification is well satisfied. And it is clear that the  $|\gamma_i| < 1$  for  $i = 1, \dots, 6$ . Thus, the notch filter is a stable filter. (A MATLAB program for the design of a notch filter is given in the Appendix.)

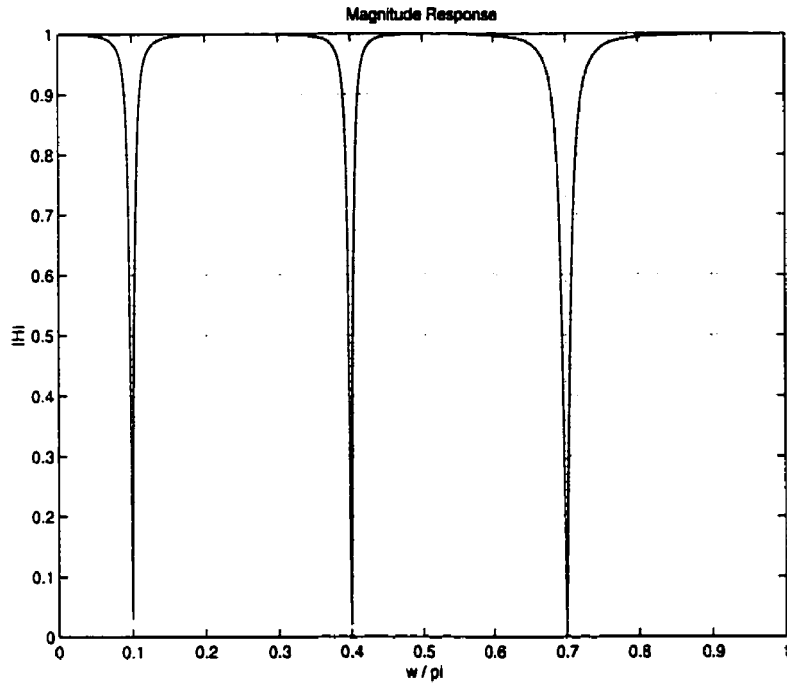


Fig. 3.5 (a) The magnitude response of the notch filter.

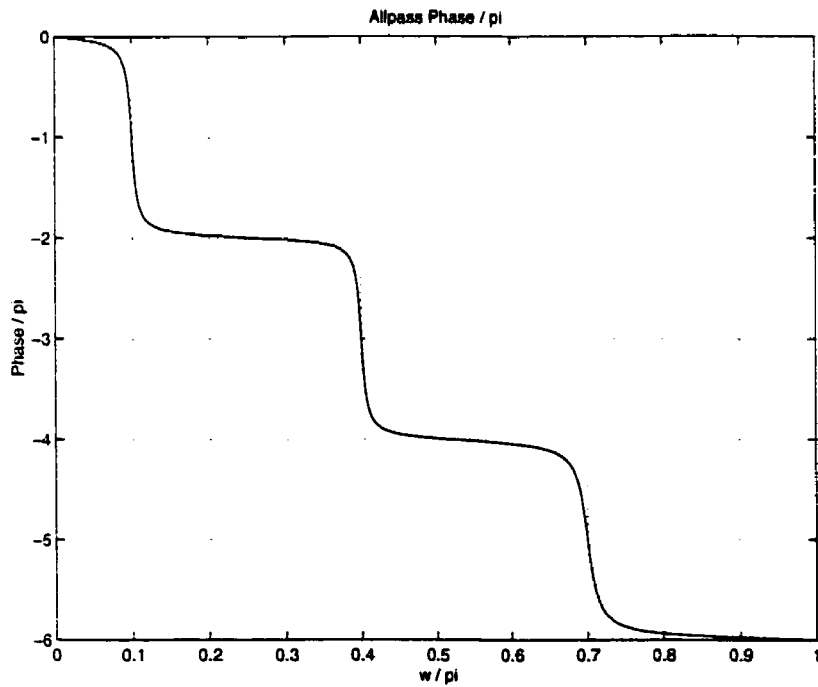


Fig. 3.5 (b) The phase response of the allpass filter.

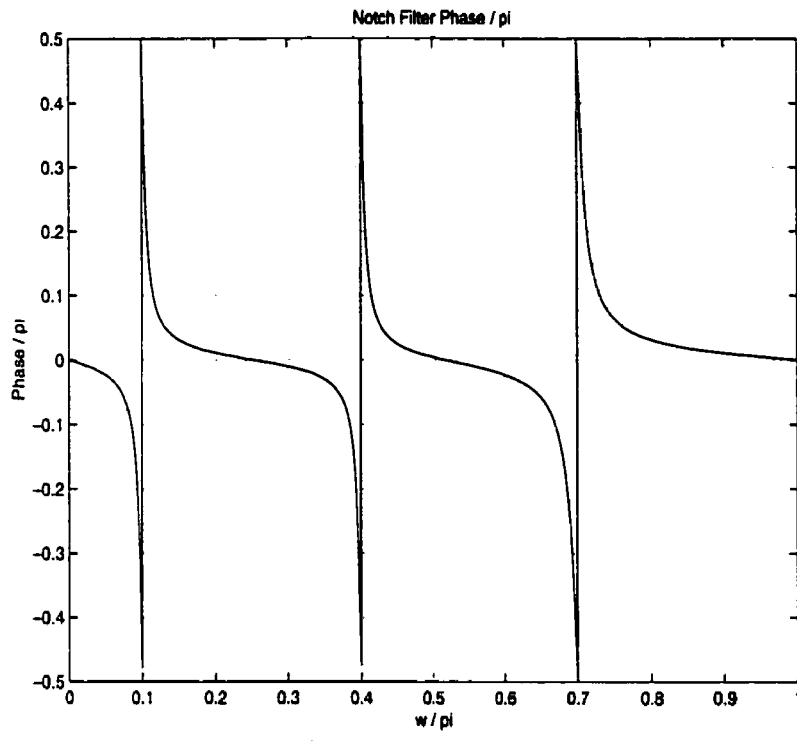


Fig. 3.5 (c) The phase response of the notch filter.

# **Chapter 4**

## ***High speed narrow-band and wide-band filter design***

Narrow-band and wide-band filters are widely used for removing low frequency noise and line frequency interference, for example, from an ECG signal. In this chapter, we will first introduce the IFIR technique, then based on this technique, we will describe the detailed design methods for both linear and nonlinear phase narrow-band and wide-band filters. In order to demonstrate these design procedures, several examples are presented.

### **4.1 The interpolated FIR (IFIR) method**

The IFIR (interpolated FIR) method [18, 19] was proposed for the efficient design of narrow-band sharp-transition FIR filters since direct FIR designs generally require very high order when the transition bandwidth is very narrow. Typically, the filter order,  $N$ , is proportional to  $1/\Delta f$ , where  $\Delta f$  is the transition bandwidth. To explain the basic idea, consider Fig. 4.1(a) which shows a narrow-band lowpass specification. Instead of meeting this specification, we try to meet a two-fold stretched specification; Fig. 4.1(b) shows the magnitude response of this stretched filter called  $G(z)$ . Note, the stretched filter  $G(z)$  has transition band width  $2\Delta f$  so that its order is  $N/2$ . Fig. 4.1(c) shows the magnitude

response of  $G(z^2)$ , where the passband around  $\pi$  is unwanted and can be suppressed by cascading  $G(z^2)$  with a new filter  $I_1(z)$  (see Fig.4.1(d)). This filter has a very wide transition band so that it requires very low order. The desired response is obtained by cascading  $G(z^2)$  and  $I_1(z)$ .

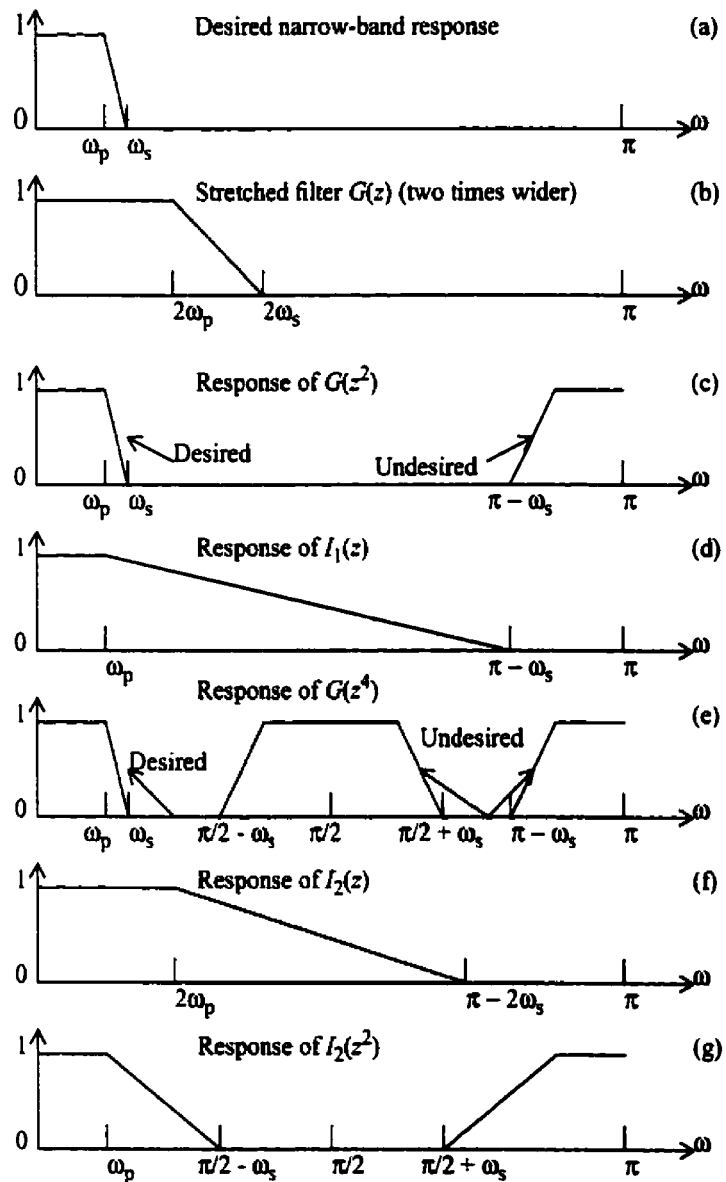


Figure 4.1 The IFIR technique for efficient design of narrowband filters



**Extensions.** Instead of stretching the specifications by two, it is possible to stretch by an amount  $M > 2$ . In principle  $M$  can be as large as the integer-part of  $\pi/\omega_s$ . Here, we consider only the case where  $M$  is a power of 2.

Consider Fig. 4.1(e) which shows  $G(z^4)$ , i.e.,  $M = 4$ .  $G(z^4)$  has two unwanted passbands. Instead of designing a FIR filter with passband edge =  $\omega_p$ , stopband edge =  $\pi/2 - \omega_s$ , we design two FIR filters. The first filter  $I_1(z)$  removes the unwanted passband around  $\pi$ , and is the same as  $I_1(z)$  in Fig. 4.1(d). Next, we need to remove the unwanted passband around  $\pi/2$ .  $I_2(z)$  is designed with passband edge =  $2\omega_p$ , and stopband edge =  $\pi - 2\omega_s$ . (see Fig. 4.1(f)). Fig. 4.1(g) shows  $I_2(z^2)$ . The desired response is obtained by cascading  $G(z^4)$ ,  $I_1(z)$  and  $I_2(z^2)$ . Notice that the passband around  $\pi$  in  $I_2(z^2)$  has no effect since the unwanted passband around  $\pi$  in Fig. 4.1(e) was already removed by  $I_1(z)$ .

This idea can be readily extended to higher  $M$ , as long as

$$M \leq \pi/\omega_s \quad (4.1)$$

For a given  $M$ , the required number of FIR filters is

$$numb = \log_2 M \quad (4.2)$$

and the  $i$ -th FIR filter is in the form of  $I_i(z^{[i]})$ , where  $[i] = 2^{i-1}$ . The passband and stopband edges of  $I_i(z)$  are

$$\omega_{pi}T = 2^{i-1} \cdot \omega_pT, \quad \omega_{si}T = \pi - 2^{i-1} \cdot \omega_sT \quad (4.3)$$

Figure. 4.2 shows the filter diagram

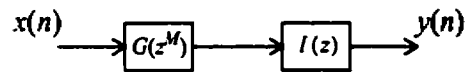


Figure. 4.2 Block diagram for IFIR narrow-band filters.

The transfer function for this filter is

$$H(z) = G(z^M)I(z) \quad (4.4)$$

where  $G(z)$  is called the model filter, and  $I(z)$  was originally called an interpolator, in here, we call it a masking filter [18], respectively. The masking filter extracts the desired image, and removes the undesired images.

As the value of  $M$  increases, the required filter order for  $G(z)$  decreases, since the new transition bandwidth of  $G(z)$  is  $M$  times wider than the original one, but if  $M$  is too large, then the transition band of  $I(z)$  becomes very narrow (so that  $I(z)$  dominates the cost), and we begin to get decreasing returns. Summarizing, as  $M$  increases the cost of  $G(z)$  decreases and that of  $I(z)$  increases. The maximum possible value of  $M$  needs to be chosen carefully based on (4.1).

## 4.2 Nonlinear phase narrow-band and wide-band filter design

In this section, based on IFIR the technique, we will present both narrow-band and wide-band filter designs.

### 4.2.1 Nonlinear phase narrow-band filter design[20]

Recursive infinite impulse-response (IIR) digital filters require, in general, a smaller

number of arithmetic operations per sample than their nonrecursive finite impulse response (FIR) counterparts. Instead of designing an FIR model filter and a masking filter, we use an IIR filter design method (described in chapter 2) for the model filter  $G(z)$  and an IIR birciprocal filter for masking filter  $I(z)$ , since elliptic approximation is more efficient than the other approaches (such as Chebyshev, Inverse-Chebyshev and Butterworth) in that the transition between passband and stopband is steeper for a given order, we use elliptic and birciprocal elliptic filters for the model filter and the masking filters (as described in chapter 2).

- **Maximal sample frequency analysis**

The maximal sample frequency for an IIR filter described by a fully specified signal flow graph, is defined [21] by

$$f_{max} = \min_i \left\{ \frac{N_i}{T_{opi}} \right\} \quad (4.5)$$

where  $T_{opi}$  is the total latency of the arithmetic operations, and  $N_i$  is the number of delay elements in the directed loop  $i$ . The loop that determines the maximal sample frequency is called the critical loop. Digital filters with high maximal sample frequencies are important for high speed applications and low power consumption, since if the required sample frequency is lower than the maximal sample frequency, then the excess speed may be utilized to reduce the power consumption [22], [23].

According to Johansson and Wanhammar [20], the maximal sample frequency for the first-order section (see Fig. 4.3) is

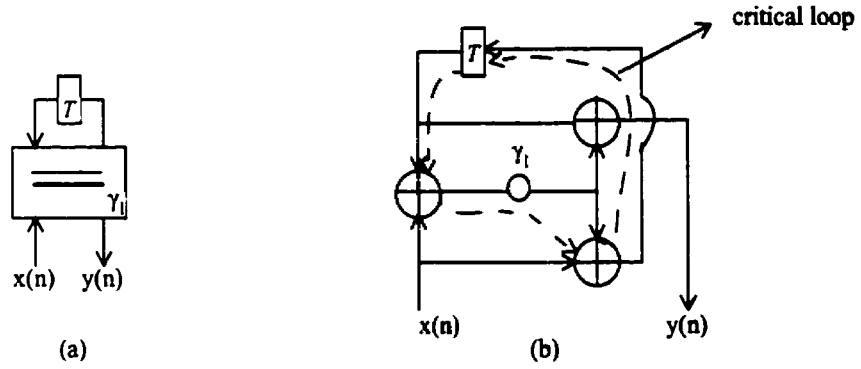


Fig. 4.3 (a) First order allpass section (b) Corresponding signal flow graph.

$$f_{max} = \frac{1}{T_{min}} = \frac{1}{T_{mult} + 2T_{add}} \quad (4.6a)$$

For the second order section (see Fig.4.4), it is

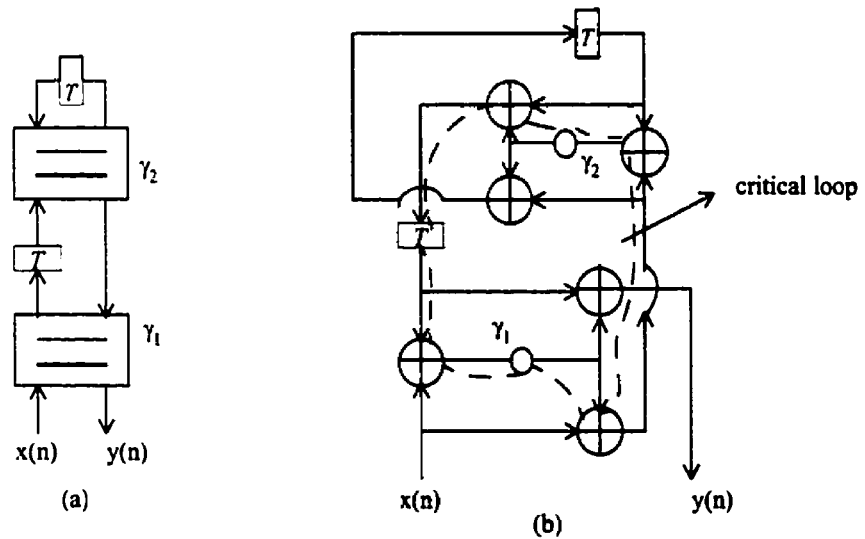


Fig. 4.4 (a) Second order allpass section (b) Corresponding signal flow graph.

$$f_{max} = \frac{1}{T_{min}} = \frac{1}{2T_{mult} + 4T_{add}} \quad (4.6b)$$

The maximal sample frequency for the allpass sections of a birciprocal filter is

$$f_{max} = \frac{1}{T_{min}} = \frac{2}{T_{mult} + 2T_{add}} \quad (4.6c)$$

From (4.5), we see two ways to increase the maximal sample frequency, the first is to reduce the latency in the critical loop, whereas the second is to increase the number of delay elements in the critical loop. The latency can be reduced by using low-sensitivity filters, and by removing unnecessary operations in the critical loop [23], [24]. However, in this chapter we are mainly concerned with the approach of increasing the number of delay elements in the critical loop, we achieve this by using the interpolated technique, an  $M$ -fold increase of the maximal sample frequency is automatically obtained, since the corresponding realization for the  $M$ -fold transfer function has at least  $M$  delay elements in its critical loop.

• **Narrow-band filter structure**

Since IIR filters can be implemented in the form of a parallel interconnection of two all-pass filters, and combined with the narrow-band block diagram shown in Fig. 4.2, we get the IIR narrow-band filter structure shown in Fig. 4.5.

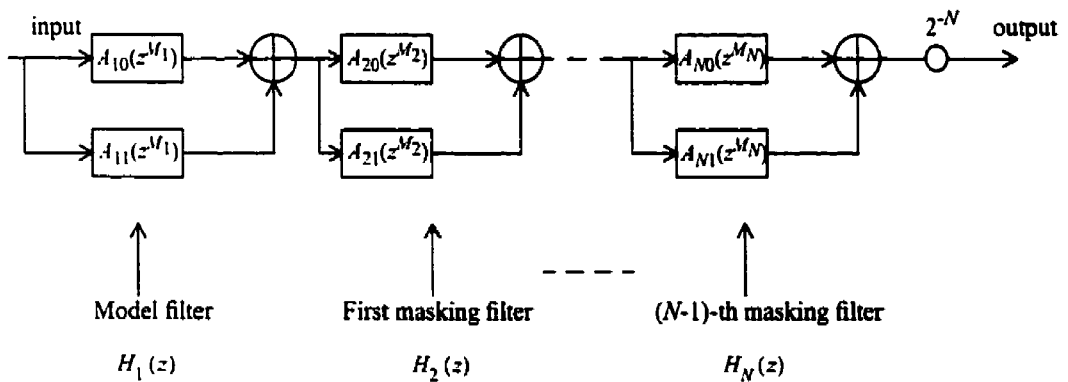


Fig. 4.5 Structure for IIR narrow-band filtering.

where  $A_{N0}$  is one of the allpass branches which can be implemented as a cascade of one first-order allpass section and a number of second-order allpass sections, whereas  $A_{N1}$  the other branch can be realized as a cascade of a number of second-order sections (see chapter 2 for details).  $H_1(z)$  is called a model filter,  $H_2(z)$  is called the first masking filter, while  $H_N(z)$  is called the  $(N-1)$ -th masking filter.

### • Design of narrow-band lowpass filters

First, let  $\omega_c T$ ,  $\omega_s T$ ,  $\delta_c$ , and  $\delta_s$  denote the passband and stopband edges and ripples, then the specification of the overall narrow-band lowpass filter is

$$\begin{aligned} 1 - \delta_c &\leq |H(e^{j\omega T})| \leq 1, & \omega T \in [0, \omega_c T] \\ |H(e^{j\omega T})| &\leq \delta_s, & \omega T \in [\omega_s T, \pi] \end{aligned} \quad (4.7)$$

Further, let  $\omega_{ci} T$  and  $\omega_{si} T$  where  $i = 1, 2, \dots, N$ , denote the passband and stopband edges of the model and masking filters.

For the model filter, we have

$$\omega_{c1} T = M_1 \omega_c T, \quad \omega_{s1} T = M_1 \omega_s T \quad (4.8)$$

i.e.,  $M_1$  times wider than that of overall narrow-band filter, and  $M_1$  should satisfy (4.1).

We also restrict  $M_1$  to be some power of two, i.e.,

$$M_1 = 2^{N-1}, \quad M_1 \leq \pi/\omega_s \quad (4.9)$$

The masking filters:

Once  $M_1$  is determined (by using (4.9)), the number of masking filters is obtained by

(4.2), i.e.,

$$N-1 = \log_2 M_1 \quad (4.10)$$

and if the parameter  $M_2$  is chosen properly, then by using a bireciprocal lattice WDFs for the masking filters, the model and masking filters will have about the same maximal sample frequency.

Comparing (4.6b,c), we get

$$M_i \geq M_1/4 \quad (4.11)$$

where  $i = 2, \dots, N$ .

Summarizing the above, we get [20]

$$M_2 = \frac{M_1}{2}, \quad M_3 = \frac{M_1}{4}, \quad M_i = \frac{M_1}{4} + 2^{N-i}, \quad i = 4, \dots, N \quad (4.12)$$

and

$$\omega_{si}T = \pi - \frac{M_i}{M_1} \left( \frac{\omega_{c1}T + 2\omega_{s1}T}{3} \right), \quad \omega_{ci}T = \pi - \omega_{si}T \quad (4.13)$$

where  $i = 2, \dots, N$ .

To see how the stopband edges of the masking filters should be chosen, first we let  $N = 3$ , then from (4.9) and (4.12), we have  $M_1 = 4$ ,  $M_2 = 2$  and  $M_3 = 1$ . Typical magnitude functions of the model and masking filters are as shown in Fig. 4.6

The model filter  $H_1(z^4)$  exhibits two unwanted images centered on  $\pi/2$  and  $\pi$  (see Fig. 4.6(b)). These two unwanted images are removed by the two masking filters. The first masking filter

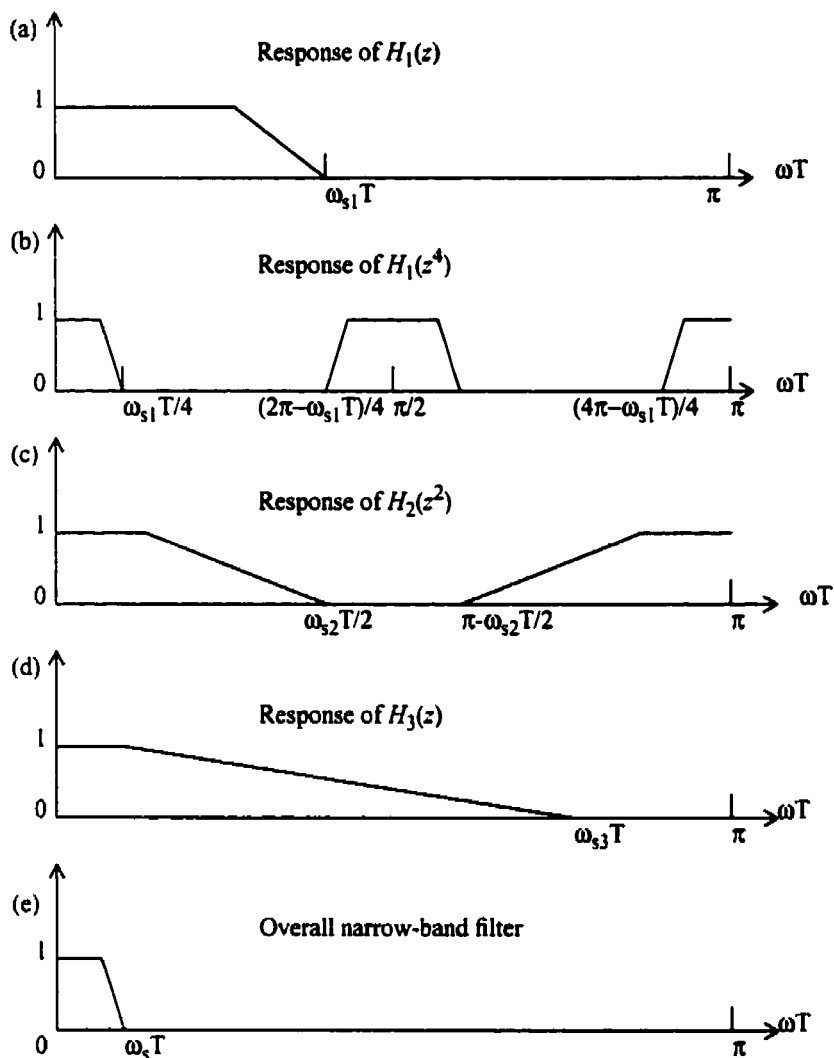


Fig. 4.6

$H_2(z^2)$  removes the image centered at  $\pi/2$ , while the second masking filter  $H_3(z)$  removes the remaining image centered at  $\pi$ .

The specified stopband attenuation of the overall filter will be satisfied by selecting the stopband attenuations of the model filter and all masking filters to equal that of the overall filter. The passband ripple of a birectiprocal lattice WDF is very small if its stopband attenuation is reasonably high. Therefore, it is possible in most practical cases to let the model



filter have the same passband ripple as that of the overall filter, i.e. model filter  $H_1(z)$  and masking filters  $H_i(z)$  satisfy:

$$1 - \delta_c \leq |H_1(z)| \leq 1, \quad \omega T \in [0, M_1 \omega_c T]$$

$$|H_1(z)| \leq \delta_s, \quad \omega T \in [M_1 \omega_s T, \pi] \quad (4.14a,b)$$

$$|H_i(z)| \leq \delta_s, \quad \omega T \in [\omega_{si} T, \pi] \quad (4.15)$$

### • Summary of design procedure

We summarize the narrow-band filter design procedure as follows:

- 1) Determine the specifications for the model filter: Choose  $M_1$  by using (4.1), then determine the passband and the stopband edges by using (4.8), and choose the passband ripple and the stopband attenuation by using (4.14a,b).
- 2) Determine the specifications for the masking filters: First, use (4.10) to select the number of masking filters, then choose  $M_i$  by using (4.12), and choose the passband and the stopband edges by using (4.13), then choose stopband attenuation by using (4.15).
- 3) Using the design method described in Chapter 2, design the model filter and the masking filters.
- 4) Cascade the model filter and the masking filters by using the structure as shown in Fig. 4.5 and obtain the overall narrow-band filter.

#### 4.2.2 Nonlinear phase wide-band filter design [20]

A wide-band filter is complementary to a narrow-band filter, since we want the delays in each branch to be approximately equal, we select one of the allpass subfilters of each lat-

tice WDF and cascade these to obtain the overall allpass filter. The wide-band filter structure is shown in Fig. 4.7.

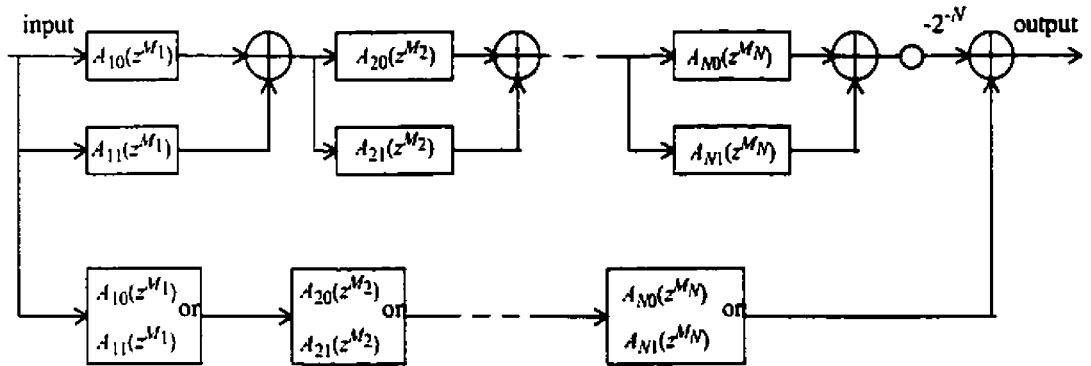


Fig. 4.7(a) Structure for IIR wide-band filtering.

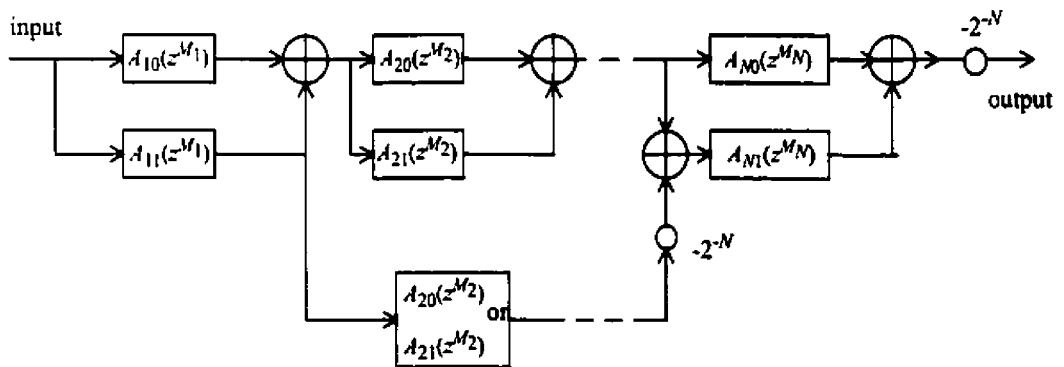


Fig. 4.7(b) Simplified structure for IIR wide-band filtering.

To obtain a wide-band filter, we first design a narrow-band filter as described in the previous section. If the narrow-band filter is a lowpass filter with passband and stopband edges  $\omega_c T$  and  $\omega_s T$ , then, by connecting this filter in parallel with a series of allpass filters, we obtain a wide-band high-pass filter with passband and stopband edges  $\omega_s T$  and

$\omega_c T$ . The passband and stopband ripples can be selected by [20]

$$|H(z)|^2 \leq 2N^2\delta_c, \quad \omega T \in \Omega_s \quad (4.16)$$

where  $\delta_c$  denotes the passband ripple of the corresponding narrow-band filter,  $\Omega_s$  denotes the stopband region of wide-band filter, and

$$1 - \delta_c \leq |H(z)| \leq 1 + \delta_c, \quad \omega T \in \Omega_c \quad (4.17)$$

where  $\Omega_c$  denotes the passband region, and  $\delta_c$  is

$$\delta_c = \max \{ \delta_{s_i} \}, \quad i = 1, 2, \dots, N. \quad (4.18)$$

The passband ripple of a narrow-band filter in the worst case is the sum of the passband ripples of the model and masking filters. Experience also shows:

$$A_{np} = A_{cp}/N, \quad A_{ns} = NA_{cs} \quad (4.19)$$

where  $A_{np}$ ,  $A_{ns}$  denote the passband ripple and stopband attenuation of the narrow-band filter, whereas  $A_{cp}$ ,  $A_{cs}$  are passband and stopband ripples of the complementary wide-band filter,  $N$  is the total number of model and masking filters.

To achieve a reasonably high stopband attenuation for the wide-band filter, the passband ripples of the model and masking filters must be very small. Due to the interdependency between the passband and stopband ripples of the masking filters, the stopband attenuation of these filters will, in most practical cases, be high enough. Therefore, the passband ripple of the wide-band filter will, in practice, be determined by the stopband ripple of the model filter.

After choosing the passband and stopband ripples of the corresponding narrow-band fil-

ter, we can use the narrow-band filter design procedure to design the corresponding narrow-band filter, and the wide-band filter can be obtained by using the structure as shown in Fig. 4.7(b).

### 4.3 Linear phase narrow-band and wide-band filter design

In some applications, a small phase deviation from a linear phase in the passband is required. In this section, we will present approximately linear phase narrow-band and wide-band filter designs.

#### 4.3.1 Linear phase narrow-band filter design [25]

This design method is also based on the IFIR technique, the model filter is designed using the approximately linear phase IIR filter design method in [26]. The IIR section is composed of a parallel connection of an allpass filter and a pure delay term. Then the IIR section is followed by FIR filters whose transition bandwidths are very wide. Due to the wide transition bandwidths, the FIR filters can be implemented without multipliers by using MF (Maximally Flat) FIR filters [27].

- **Model filter design**

For linear-phase lattice WDFs, there exist no closed-form solutions for computation of the adaptor coefficients. Therefore, numerical optimization algorithms must be used.

- 1) Constructing the magnitude function

Since the model filter is composed of a parallel connection of an allpass filter and a pure delay term, we can write the transfer function as

$$H(z) = \frac{1}{2} \left[ z^{-M_1} + A_{M_2}(z) \right] \quad (4.3.1)$$

where  $A_{M_2}(z)$  is an allpass transfer function, and can be written as

$$A_{M_2}(e^{j\omega}) = e^{j\phi(\omega)}$$

then (4.3.1) can be written as

$$\begin{aligned} H(e^{j\omega}) &= \frac{1}{2} \left( e^{-jM_1\omega} + e^{j\phi(\omega)} \right) \\ &= e^{j\frac{1}{2}(\phi(\omega) - M_1\omega)} \cos \frac{1}{2}(\phi(\omega) + M_1\omega) \end{aligned}$$

that is

$$\left| H(e^{j\omega}) \right| = \left| \cos \frac{1}{2}(\phi(\omega) + M_1\omega) \right| \quad (4.3.2)$$

and the magnitude should be bounded:

$$1 - \delta_p \leq \left| H(e^{j\omega}) \right| \leq 1, \quad \omega \in [0, \omega_p]$$

$$\left| H(e^{j\omega}) \right| \leq \delta_s, \quad \omega \in [\omega_s, \pi] \quad (4.3.3)$$

2) Transform the filter specifications to allpass phase specifications:

We also can write allpass filter  $A_{M_2}(z)$  for  $z = e^{j\omega}$  as

$$A_{M_2}(e^{j\omega}) = \frac{\sum_{k=0}^{M_2} a_k e^{-j\omega(M_2-k)}}{\sum_{k=0}^{M_2} a_k e^{-j\omega k}} \quad (4.3.4)$$

If  $\phi$  denotes the phase of  $A_{M_2}(e^{j\omega})$ , and  $\phi_1$  denotes the phase of the denominator of

(4.3.4), then, we have (see Chapter 3 for proof)

$$\phi_1 = -\tan^{-1} \left( \frac{\sum_{k=0}^{M_2} a_k \sin \omega k}{\sum_{k=0}^{M_1} a_k \cos \omega k} \right) \quad (4.3.5a)$$

Also

$$\phi_1 = -\frac{1}{2} (M_2 \omega + \phi) \quad (4.3.5b)$$

and from (4.3.2), we get

$$\phi(\omega) = -M_1 \omega + 2 \cos^{-1} |H(e^{j\omega})| \quad (4.3.6)$$

substitute (4.3.6) to (4.3.5), we get

$$\phi_1(\omega) = -\frac{1}{2} (M_2 \omega - M_1 \omega + 2 \cos^{-1} |H(e^{j\omega})|) \quad (4.3.7)$$

3) Formulate the error function

The error function to be minimized is

$$E(\omega) = W(\omega) [\phi(\omega) - D(\omega)] \quad (4.3.8)$$

where

$$W(\omega) = \left( \begin{array}{l} \frac{1}{2 \cos^{-1} (1 - \delta_p(\omega))}, \quad \omega \in [0, \omega_p] \\ \frac{1}{2 \sin^{-1} (\delta_s(\omega))}, \quad \omega \in [\omega_s, \pi] \end{array} \right) \quad (4.3.9)$$

and

$$D(\omega) = \begin{cases} -M_1 \omega, & \omega \in [0, \omega_p] \\ -M_1 \omega + \pi, & \omega \in [\omega_s, \pi] \end{cases} \quad (4.3.10)$$

4) Algorithm [26]

Step 1. Initialize  $\omega_p$ ,  $\omega_s$ ,  $\delta_p$ ,  $\delta_s$ ,  $M_1$ , and  $M_2$ .

Step 2. Select the number of passband extremal points

$$n = (M_2 + 1) \omega_p / (\omega_p + \pi - \omega_s), \text{ rounded to the nearest integer. After}$$

selecting the number of passband extremal points, the extremal points can be selected to lie equidistantly on the passband and stopband regions.

Step 3. Select initial extremal points.  $\Omega = \{\omega_1, \omega_2, \dots, \omega_{M_2+1}\}$  on the passband and

the stopband. According to the number of passband extrema points, the extrema points can be selected to lie equidistantly on the passband and stopband regions.

Step 4. Solve for  $\phi$  from

$$E(\omega_j) = W(\omega_j) [\phi(\omega_j) - D(\omega_j)] = (-1)^j \delta, \quad j = 1, 2, \dots, M_2 + 1$$

using (4.3.5b) get  $\phi_1$ , then solve (4.3.5a) to get filter coefficients  $a_1, a_2, \dots, a_{M_2}$ , and then solve for  $\delta$ .

Step 5. Built up error function  $E(\omega)$ , and find  $M_2 + 1$  local extrema whose absolute values are the largest with the condition that the maxima and minima alternate.

Store the abscissa of the extrema into  $\Omega' = \{\omega'_1, \omega'_2, \dots, \omega'_{M_2+1}\}$ .

Step 6. If  $|\omega_j - \omega'_j| \leq \epsilon$  for  $j = 1, 2, \dots, M_2 + 1$ , then go to the next step. Otherwise set

$$\Omega = \Omega' \text{ and go to step 4.}$$

Step 7. Compute  $H(z)$  and give the frequency response of the filter.

### • Masking filter design

In this part, we will use the MF (Maximally Flat) linear phase FIR approach to design masking filters.

The MF FIR transfer function can be written as [27]:

$$H(z) = \left(\frac{1+z^{-1}}{2}\right)^{2K} \cdot \sum_{n=0}^{L-1} z^{-(L-1-n)} (-1)^n d(n) \left(\frac{1-z^{-1}}{2}\right)^{2n} \quad (4.3.11)$$

where

$$d(n) = \frac{(K-1+n)!}{(K-1)!n!} \quad (4.3.12)$$

where  $K, L$  can be determined from the filter specification [28] (there is a program in [28] to compute  $K$  and  $L$ ).

And filter order  $N, K$ , and  $L$  are related by

$$N = 2(K+L-1) \quad (4.3.13)$$

Thus for a given  $N$  and  $K, L$  represents the maximum degree of flatness at  $\omega = 0$ . Similarly, for a given  $N$  and  $L, K$  represents the maximum degree of flatness at  $\omega = \pi$ .

It should be mentioned: The number of masking filter can be determined by using (4.10), and the passband and stopband edges can be determined by using (4.3).

#### 4.3.2 Linear phase wide-band filter design

A wide-band high-pass filter is the complementary filter to a narrow-band lowpass filter, and can be obtained by using the structure as shown in Fig.4.8



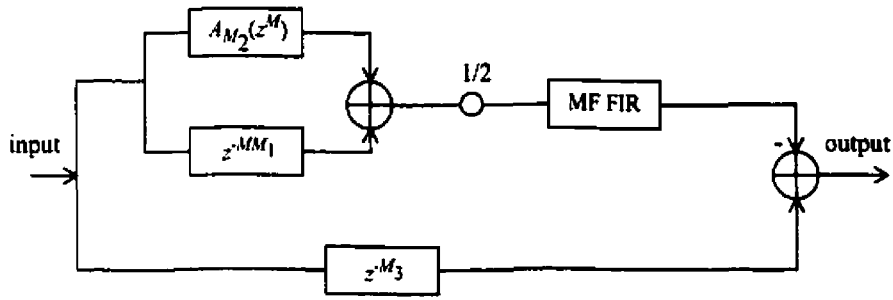


Fig. 4.8 The structure for wide-band high-pass filter.

where  $M_3$  can be determined by  $M$  and  $M_1$ , and the length of MF FIR filters.

#### 4.4 Roundoff noise analysis for interpolated WDFs

The roundoff noise can be measured by NSR (Noise to signal ratio), and the NSR for first-order and second-order allpass sections is [29]

$$NSR_{1st} \propto \frac{1}{\epsilon^2}, \quad NSR_{2nd} \propto \frac{1}{\epsilon^2 \sin^2 \theta} \quad (4.4.1)$$

where  $\epsilon$  is the distance from the unit circle to the pole location, when the transition bandwidth of model filter is increased by  $M$  times, the poles generally move away from the unit circle by  $M$  times  $\epsilon$ . Therefore, by  $M$  level interpolations, the NSR of cascaded IIR filters decreases by  $M^2$  and these implementations are preferable to WDF implementations for larger  $M$ , this is an obvious conclusion obtained from (4.4.1). The roundoff noise of the model filter alone is therefore lower than for the corresponding conventional filter without taking into account the contributions of the masking filters.

## 4.5 The examples

In this section, several design examples will be presented.

*Example 1: Low-pass narrow-band filter design.*

Specification [30]:

- $\omega_c T = 0.0625\pi$  ( $11.25^\circ$ ),  $\omega_s T = 0.075\pi$  ( $13.5^\circ$ ),
- $A_{max} = 0.5\text{dB}$ ,  $A_{min} = 50\text{dB}$ .

**Method (i):** Direct design method (conventional design method):

These specifications can be met by a seventh-order elliptic filter, with the poles (in the digital domain):

$$p_{1,2} = 0.97606586 \pm 0.19500405j$$

$$p_{3,4} = 0.943864 \pm 0.11575329j$$

$$p_{5,6} = 0.96463816 \pm 0.17502166j$$

$$p_7 = 0.92874051$$

Note, these poles are close to the unit circle. Then the elliptic filter is implemented using the lattice WDF structure described in chapter 2, the adaptor coefficients can be obtained as

$$\gamma_1 = 0.92874051479306, \gamma_2 = -0.96115936623788, \gamma_3 = 0.98374275779617,$$

$$\gamma_4 = -0.90427807728677, \gamma_5 = 0.99130900282711, \gamma_6 = -0.99073114126480,$$

$$\gamma_7 = 0.98061042915654.$$

Fig. 4.10 shows the frequency response using word-lengths,  $W = 17$ .

**Method (ii):** Described method (interpolated method).

Model filter design:

Determining the specifications:

$$M_1 \leq \pi / \omega_s = 1 / 0.075 = 13.3, \text{ we choose } M_1 = 4 .$$

$$\omega_{c1} T = M_1 \omega_c T = 4 \times 0.0625\pi = 0.25\pi ,$$

$$\omega_{s1} T = M_1 \omega_s T = 4 \times 0.075\pi = 0.3\pi ,$$

$$A_{1max} = 0.5dB, A_{1min} = 50dB .$$

The specifications can be met by a seventh-order elliptic filter, with the poles (in the digital domain):

$$p_{1,2} = 0.69313023 \pm 0.69743825j$$

$$p_{3,4} = 0.69577352 \pm 0.61582191j$$

$$p_{5,6} = 0.71562121 \pm 0.39821999j$$

$$p_7 = 0.73103235$$

Note, these poles are further from the unit circle than the poles of the direct method. The adaptor coefficients can be obtained as

$$\gamma_1 = 0.73103234889104, \gamma_2 = -0.86333741466988, \gamma_3 = 0.74680357364510,$$

$$\gamma_4 = -0.67062988457961, \gamma_5 = 0.8566759592606, \gamma_6 = -0.96684962897323,$$

$$\gamma_7 = 0.70481263233903.$$

Masking filter design:

First, determine the number of masking filters =  $\log_2 M_1 = 2$  .

The first masking filter design:

Determine the specifications:

$$M_2 = \frac{M_1}{2} = \frac{4}{2} = 2,$$

$$\omega_{s2}T = \pi - \frac{M_2}{M_1} \cdot \left( \frac{\omega_{c1}T + 2\omega_{s1}T}{3} \right) = 0.8583\pi,$$

$$\omega_{c2}T = \pi - \omega_{s2}T = 0.1417\pi,$$

$$A_{2min} = 50dB.$$

The specifications can be met by a 3rd-order birciprocal elliptic filter described in chapter 2, section 2.3.2. The obtained adaptor coefficient is

$$\gamma_1 = -0.35058484219591.$$

The passband ripple and stopband attenuation are

$$A_{s2} = 50.78dB, A_{p2} = 3.62 \times 10^{-5}dB.$$

The second masking filter design:

Determine the specifications:

$$M_3 = \frac{M_1}{4} = 1,$$

$$\omega_{s3}T = \pi - \frac{M_3}{M_1} \cdot \left( \frac{\omega_{c1}T + 2\omega_{s1}T}{3} \right) = 0.9292\pi,$$

$$\omega_{c3}T = \pi - \omega_{s3}T = 0.0708\pi,$$

$$A_{3min} = 50dB.$$

The specifications can be met by an 3rd-order birciprocal elliptic filter, the obtained adaptor coefficient is

$$\gamma_1 = -0.3375033802279.$$

The passband ripple and stopband attenuation are

$$A_{s3} = 69dB, A_{p3} = 5.265 \times 10^{-7} dB.$$

The overall narrow-band filter structure is as shown in Fig. 4.9, and Fig. 4.11 shows the frequency response of the overall narrow-band filter using word-lengths,  $W = 12$ .

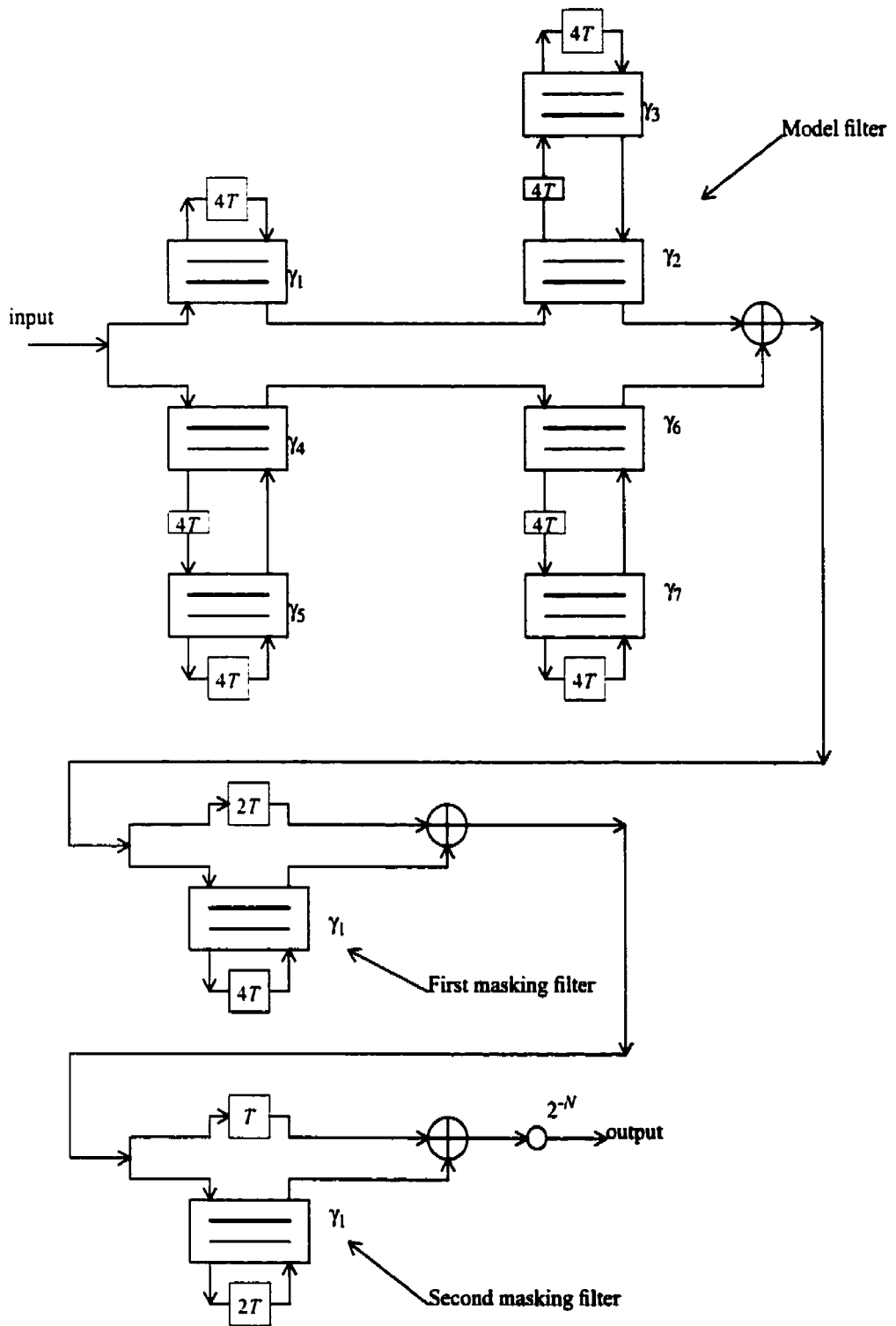


Fig. 4.9 Structure of overall narrow-band filter for example 1.

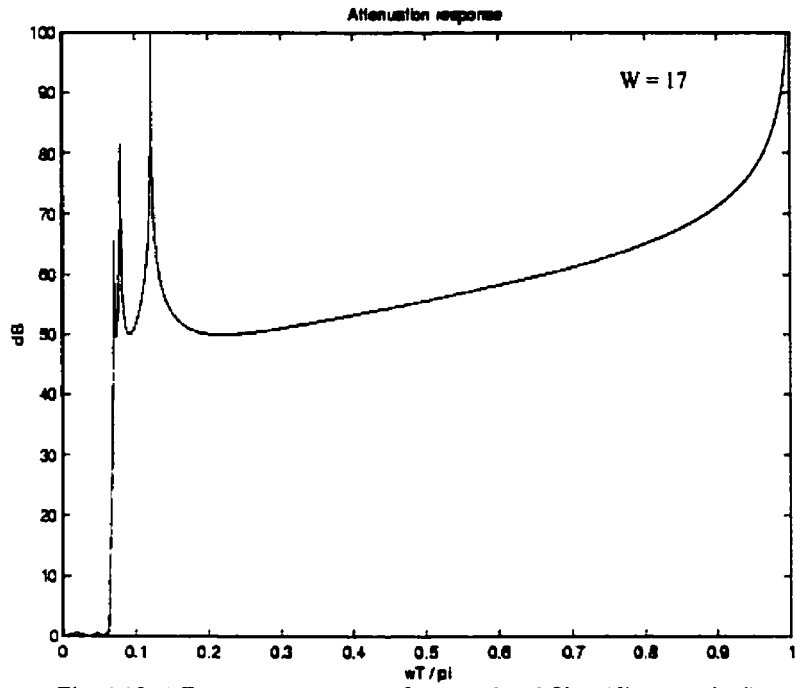


Fig. 4.10(a) Frequency response of narrow-band filter (direct method).

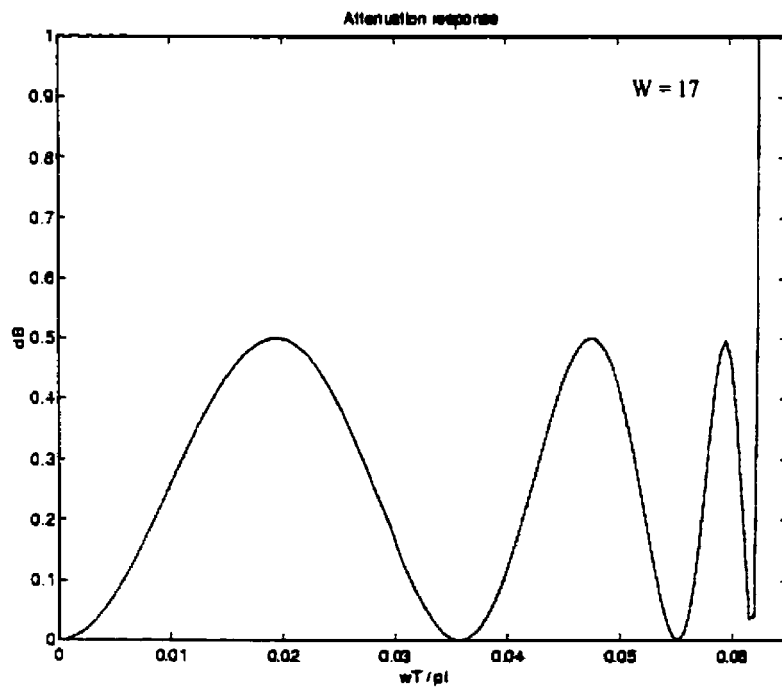


Fig. 4.10(b) Ripple response of narrow-band filter (direct method).

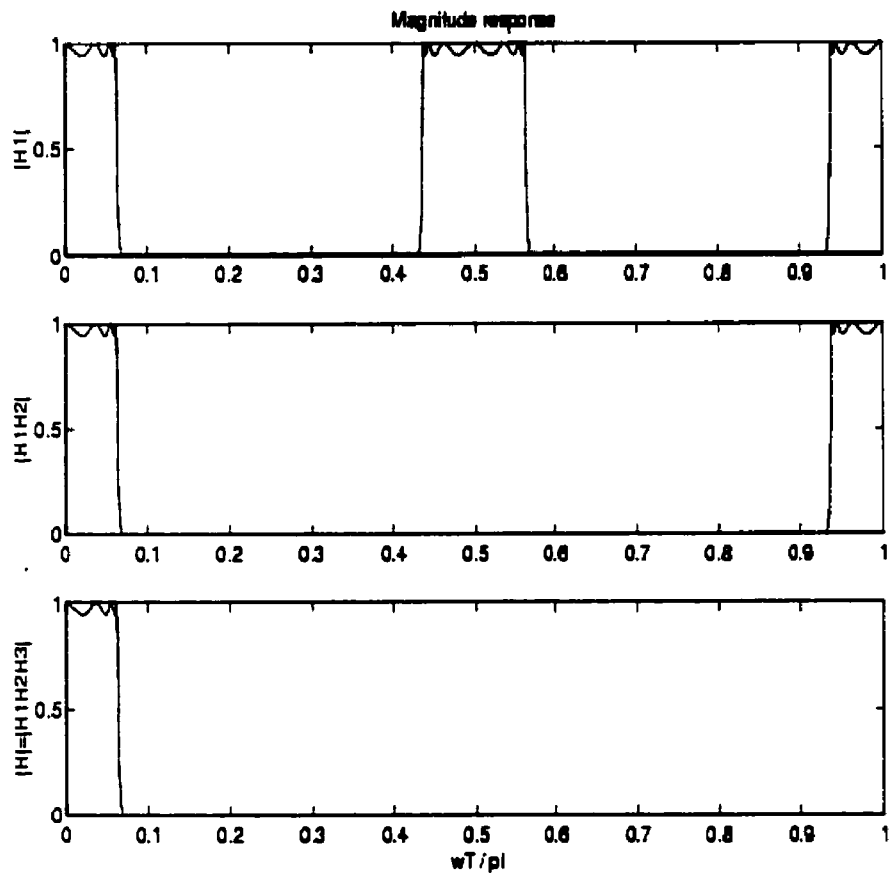


Fig. 4.11(a) Magnitude response of model filter, and cascade model filter with masking filters (for example 1, interpolated method).



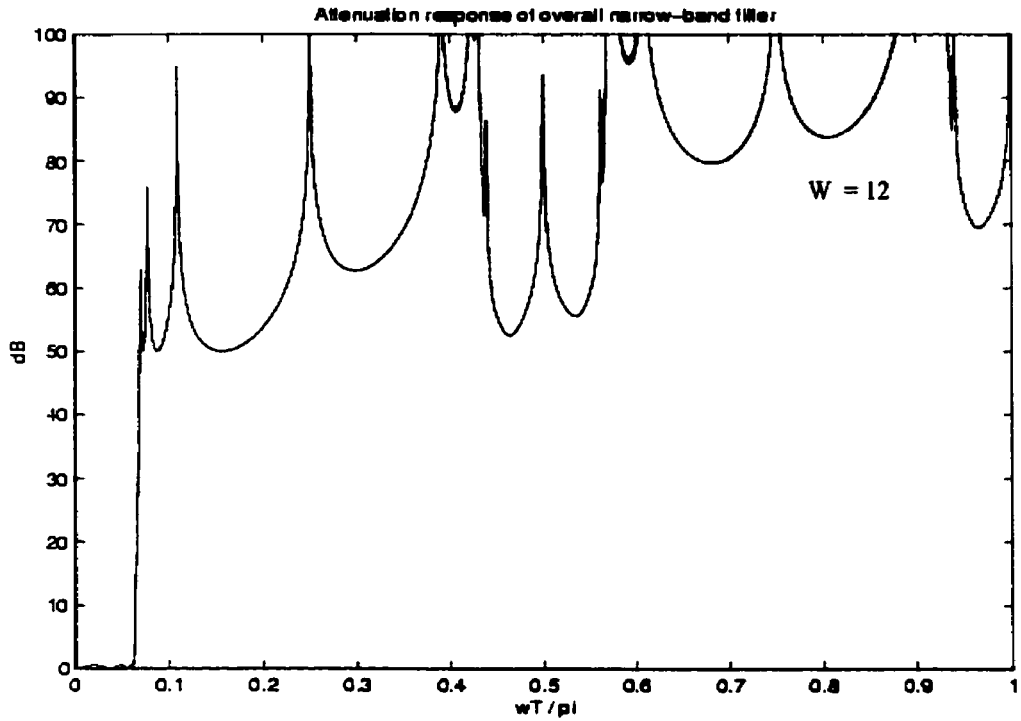


Fig. 4.11(b) Frequency response of overall narrow-band filter (interpolated method).

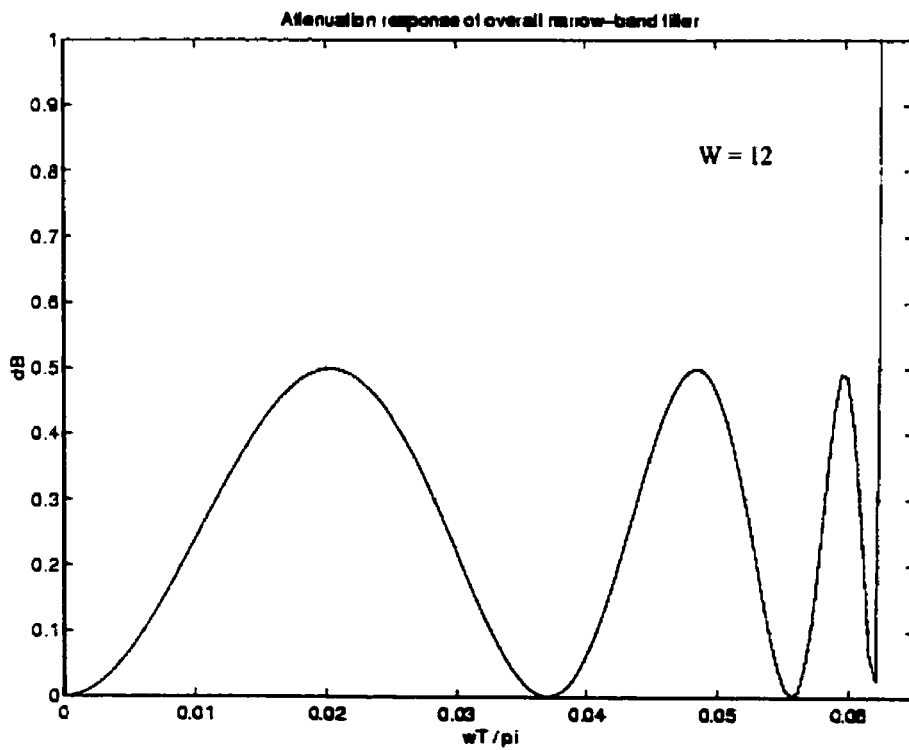


Fig. 4.11(c) Ripple response of overall narrow-band filter (interpolated method).

*Example 2: High-pass wide-band filter design.*

Specification [25]:

- $\omega_c T = 0.075\pi$  (13.5°),  $\omega_s T = 0.0625\pi$  (11.25°),
- $A_{max} = 0.2\text{dB}$ ,  $A_{min} = 50\text{dB}$ .

**Method (i): Direct design method (conventional design method):**

These specifications can be met by a seventh-order elliptic filter, with the poles (in the digital domain)

$$p_1 = 0.5911553$$

$$p_{2,3} = 0.82176043 \pm 0.25314993j$$

$$p_{4,5} = 0.93461005 \pm 0.23900864j$$

$$p_{6,7} = 0.96595755 \pm 0.22834833j$$

Then the elliptic filter is implemented using the lattice WDF structure described in chapter 2, the adaptor coefficients can be obtained as

$$\gamma_1 = 0.59115529848347, \gamma_2 = -0.93062108088553, \gamma_3 = 0.96819625800425,$$

$$\gamma_4 = -0.73937508416515, \gamma_5 = 0.94489156926825, \gamma_6 = -0.98521695086713,$$

$$\gamma_7 = 0.97315061854081.$$

Fig. 4.13 shows the frequency response using word-lengths,  $W = 17$ .

**Method (ii):** Described method (interpolated method).

Corresponding narrow-band specifications:

$$M_1 \leq \pi / \omega_s = 1 / 0.075 = 13.3, \text{ we choose } M_1 = 4.$$

Determine the total number of model filter and masking filters:

$$N = \log_2 M_1 + 1 = 3.$$

Since the specifications of the wide-band filter are  $A_{ws} = 50dB$ ,  $A_{wp} = 0.2dB$ , then

the specifications of the corresponding complementary narrow-band filter are

$$A_{cp} = 0.4343 \times 10^{-4} dB \text{ and } A_{cs} = 13.47 dB. \text{ We choose the passband and stopband rip-}$$

ples of the narrow-band filter as

$$A_{np} = \frac{A_{cp}}{N} \approx 10^{-5} dB, A_{ns} = N \cdot A_{cs} \approx 40 dB.$$

Model filter design:

Determining the specifications:

$$\omega_{c1} T = M_1 \omega_c T = 4 \times 0.0625\pi = 0.25\pi,$$

$$\omega_{s1} T = M_1 \omega_s T = 4 \times 0.075\pi = 0.3\pi,$$

$$A_{1max} = 10^{-5} dB, A_{1min} = 40 dB.$$

The specifications can be met by an 11th-order elliptic filter, with the poles (in the digital domain):

$$p_1 = 0.28671991$$

$$p_{2,3} = 0.63337773 \pm 0.70275305j$$

$$p_{4,5} = 0.57862203 \pm 0.65571435j$$

$$p_{6,7} = 0.48253878 \pm 0.55379296j$$

$$p_{8,9} = 0.35560688 \pm 0.34139427j$$

$$p_{10,11} = 0.66319926 \pm 0.72833384j$$

The adaptor coefficients can be obtained as

$$\gamma_1 = 0.28671991154392, \gamma_2 = -0.53953031878987, \gamma_3 = 0.62686492810183,$$

$$\gamma_4 = -0.89502919636046, \gamma_5 = 0.66846224032534, \gamma_6 = -0.24300630107066,$$

$$\gamma_7 = 0.57217228785650, \gamma_8 = -0.76476475528964, \gamma_9 = 0.65574975306234,$$

$$\gamma_{10} = -0.97030342888112, \gamma_{11} = 0.67319504866259.$$

Masking filter design:

First, determine the number of masking filters =  $\log_2 M_1 = 2$ .

The first masking filter design:

Determine the specifications:

$$M_2 = \frac{M_1}{2} = \frac{4}{2} = 2,$$

$$\omega_{s2}T = \pi - \frac{M_2}{M_1} \cdot \left( \frac{\omega_{c1}T + 2\omega_{s1}T}{3} \right) = 0.8583\pi,$$

$$\omega_{c2}T = \pi - \omega_{s2}T = 0.1417\pi,$$

$$A_{2min} = 40dB, A_{2max} = 10^{-5}dB.$$

The specifications can be met by an 5th-order biceiprocal elliptic filter, the obtained adaptor coefficients are

$$\gamma_1 = -0.11455485826387, \gamma_2 = -0.54458467232029.$$

The passband ripple and stopband attenuation are

$$A_{s2} = 88.66dB, A_{p2} = 5.9 \times 10^{-9}dB.$$

The second masking filter design:

Determine the specifications:

$$M_3 = \frac{M_1}{4} = 1,$$

$$\omega_{s3}T = \pi - \frac{M_3}{M_1} \cdot \left( \frac{\omega_{c1}T + 2\omega_{s1}T}{3} \right) = 0.9292\pi,$$

$$\omega_{c3}T = \pi - \omega_{s3}T = 0.0708\pi,$$

$$A_{3min} = 50dB, A_{3max} = 10^{-5}dB$$

The specifications can be met by an 3rd-order birciprocal elliptic filter, the obtained adaptor coefficient is

$$\gamma_1 = -0.3375033802279.$$

The passband ripple and stopband attenuation are

$$A_{s3} = 69dB, A_{p3} = 5.265 \times 10^{-7}dB.$$

The overall wide-band filter structure is as shown in Fig. 4.12. Fig. 4.14 shows the frequency response of overall wide-band filter using word-lengths,  $W = 11$ . (A MATLAB program for the design of a wide-band filter is given in the Appendix.)

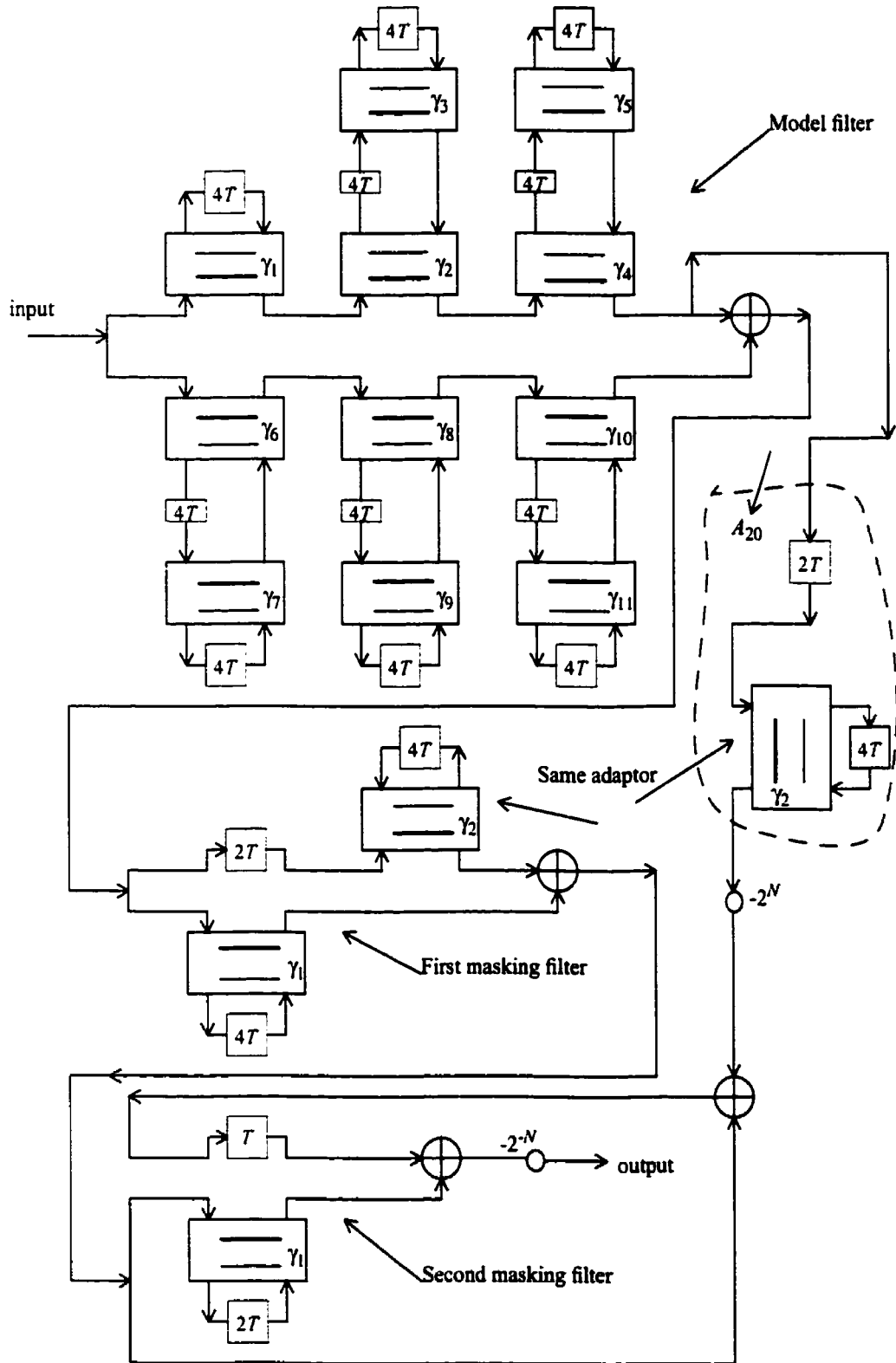


Fig. 4.12 Structure of overall wide-band filter for example 2 (interpolated method).

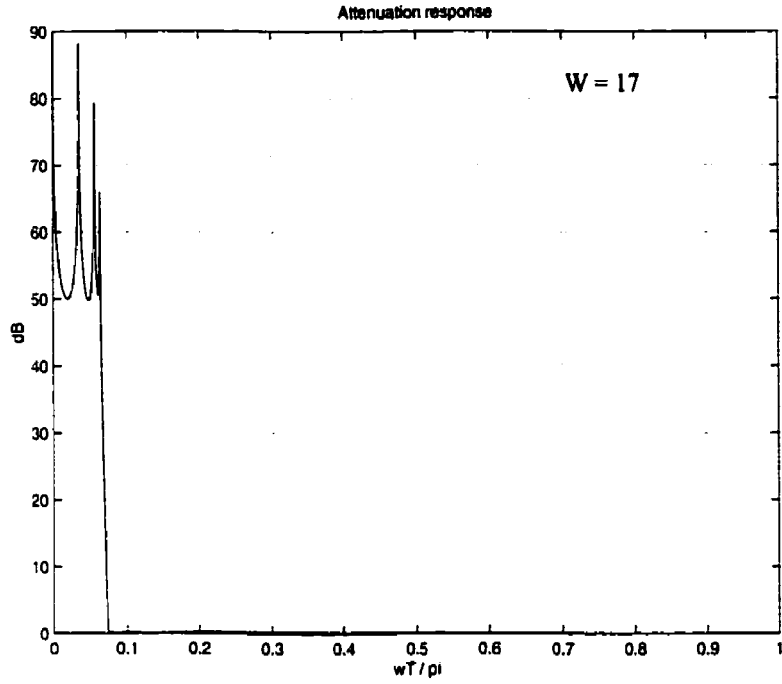


Fig 4.13(a) Frequency response of wide-band filter (direct method).

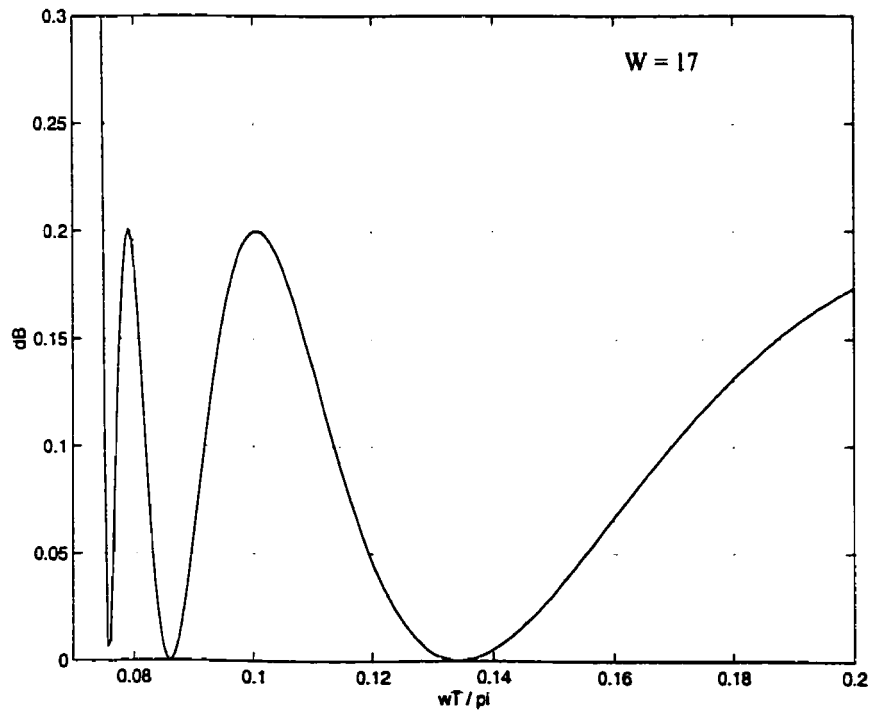


Fig 4.13(b) Ripple response of wide-band filter (direct method).

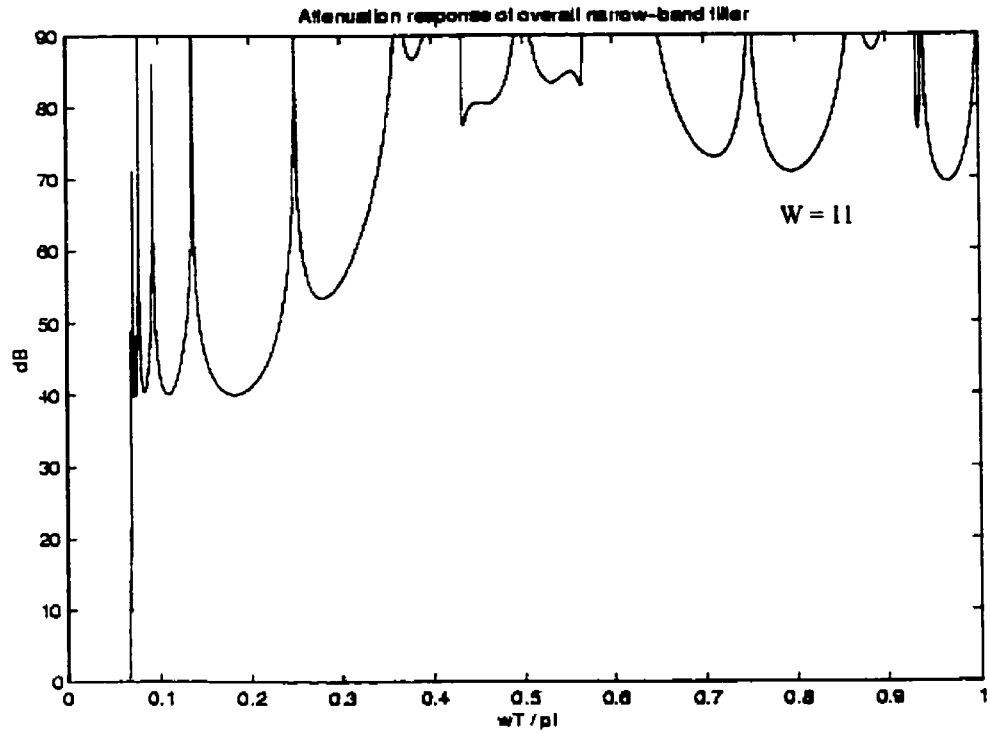


Fig. 4.14(a) Frequency response of corresponding narrow-band filter  
(interpolated method for example 2).

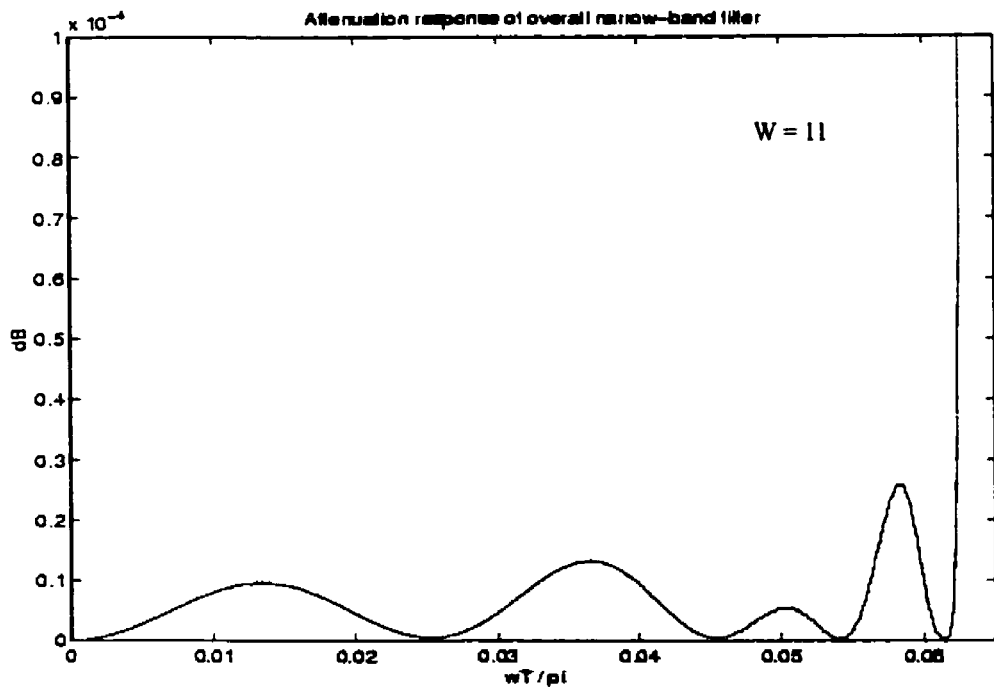


Fig. 4.14(b) Ripple response of corresponding narrow-band filter  
(interpolated method for example 2).



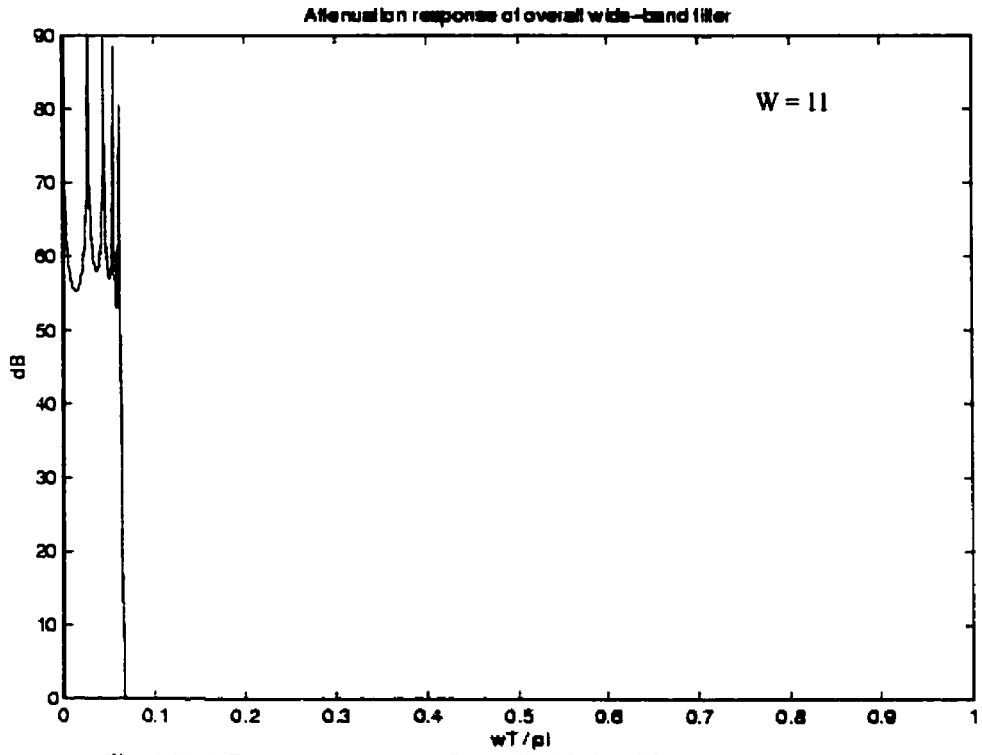


Fig. 4.14(c) Frequency response of overall wide-band filter (interpolated method).

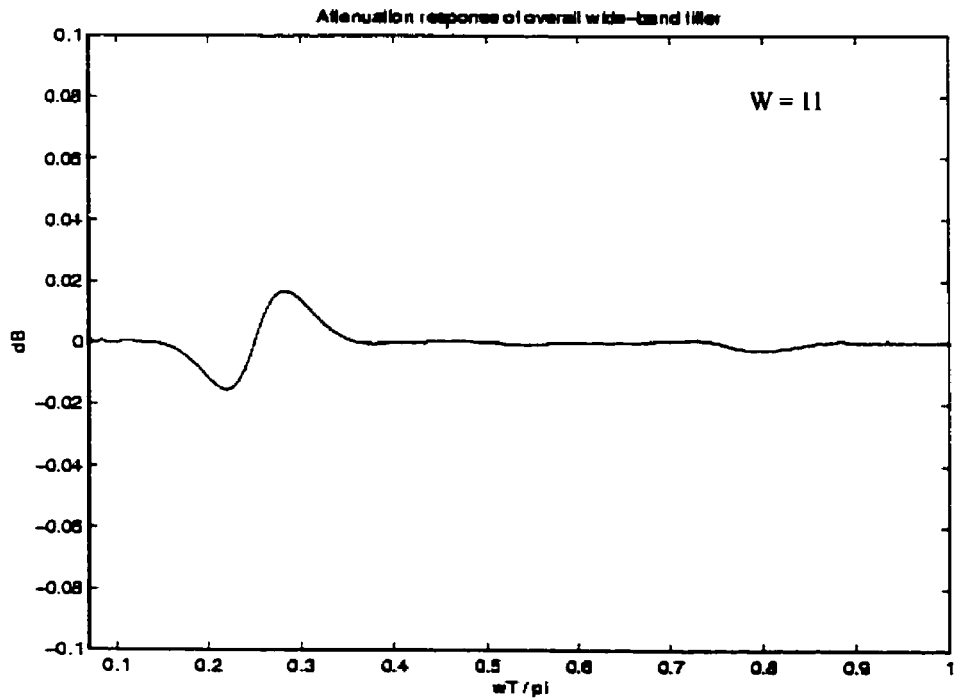


Fig. 4.14(d) Ripple response of overall wide-band filter (interpolated method).

*Example 3: Low-pass narrow-band filter design (linear phase).*

Specification:

- $\omega_c T = 0.0625\pi$  ( $11.25^\circ$ ),  $\omega_s T = 0.075\pi$  ( $13.5^\circ$ ),
- $A_{max} = 0.1\text{dB}$ ,  $A_{min} = 40\text{dB}$ .

Model filter design:

Determining the specifications:

$$M_1 \leq \pi / \omega_s = 1 / 0.075 = 13.3, \text{ we choose } M_1 = 8.$$

$$\omega_{c1} T = M_1 \omega_c T = 8 \times 0.0625\pi = 0.5\pi,$$

$$\omega_{s1} T = M_1 \omega_s T = 8 \times 0.075\pi = 0.6\pi,$$

$$A_{1max} = 0.1\text{dB}, A_{1min} = 40\text{dB}.$$

To meet the specifications, apply the method described in section 4.2.1. We get a 17th-order IIR filter (allpass degree is 9, the delay degree is 8), the allpass filter coefficients are

$$a_{1-4} = 1.000000, 0.121666, 0.487569, -0.059062,$$

$$a_{5-7} = -0.105517, 0.044379, 0.026499,$$

$$a_{8-10} = -0.081658, -0.098785, -0.029697.$$

Masking filter design:

First, determine the number of masking filters  $= \log_2 M_1 = 3$ .

The first masking filter design:

Determine the specifications:

$$\omega_{c2}T = \omega_c T = 0.0625\pi,$$

$$\omega_{s2}T = \pi - \omega_s T = 0.925\pi,$$

$$A_{2max} = 0.1dB, A_{2min} = 40dB.$$

Apply the method described in section 4.2.1 masking filter design part, the specification can be met for  $K_1 = 2, L_1 = 2$ , the transfer function for this maximally flat linear phase FIR filter is

$$I_1(z) = \left(\frac{1+z^{-1}}{2}\right)^4 \left(z^{-1} - 2\left(\frac{1-z^{-1}}{2}\right)^2\right)$$

The second masking filter design:

Determine the specifications:

$$\omega_{c3}T = 2\omega_c T = 0.125\pi,$$

$$\omega_{s3}T = \pi - 2\omega_s T = 0.85\pi,$$

$$A_{3max} = 0.1dB, A_{3min} = 40dB.$$

The specification can be met for  $K_2 = 2, L_2 = 3$ , the transfer function for this maximally flat linear phase FIR filter is

$$I_2(z) = \left(\frac{1+z^{-1}}{2}\right)^4 \left(z^{-2} - 2z^{-1}\left(\frac{1-z^{-1}}{2}\right)^2 + \left(\frac{1-z^{-1}}{2}\right)^4\right)$$

The third masking filter design:

Determine the specifications:

$$\omega_{c4}T = 4\omega_c T = 0.25\pi,$$

$$\omega_{s4}T = \pi - 4\omega_s T = 0.7\pi,$$

$$A_{4max} = 0.1dB, A_{4min} = 40dB.$$

The specification can be met for  $K_3 = 5, L_3 = 6$ , the transfer function for this Maximal flat linear phase FIR filter is:

$$I_3(z) = \left(\frac{1+z^{-1}}{2}\right)^{10} \left( z^{-5} - 5z^{-4} \left(\frac{1-z^{-1}}{2}\right)^2 + 15z^{-3} \left(\frac{1-z^{-1}}{2}\right)^4 - 35z^{-2} \left(\frac{1-z^{-1}}{2}\right)^6 + 70z^{-1} \left(\frac{1-z^{-1}}{2}\right)^8 - 126 \left(\frac{1-z^{-1}}{2}\right)^{10} \right)$$

The overall narrow-band filter structure is shown in Fig. 4.15.

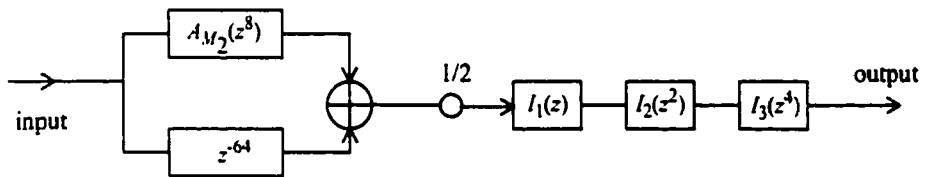


Fig. 4.15 The structure for narrow-band low-pass filter (example 3).

The frequency response of overall narrow-band filter is shown in Fig. 4.16.

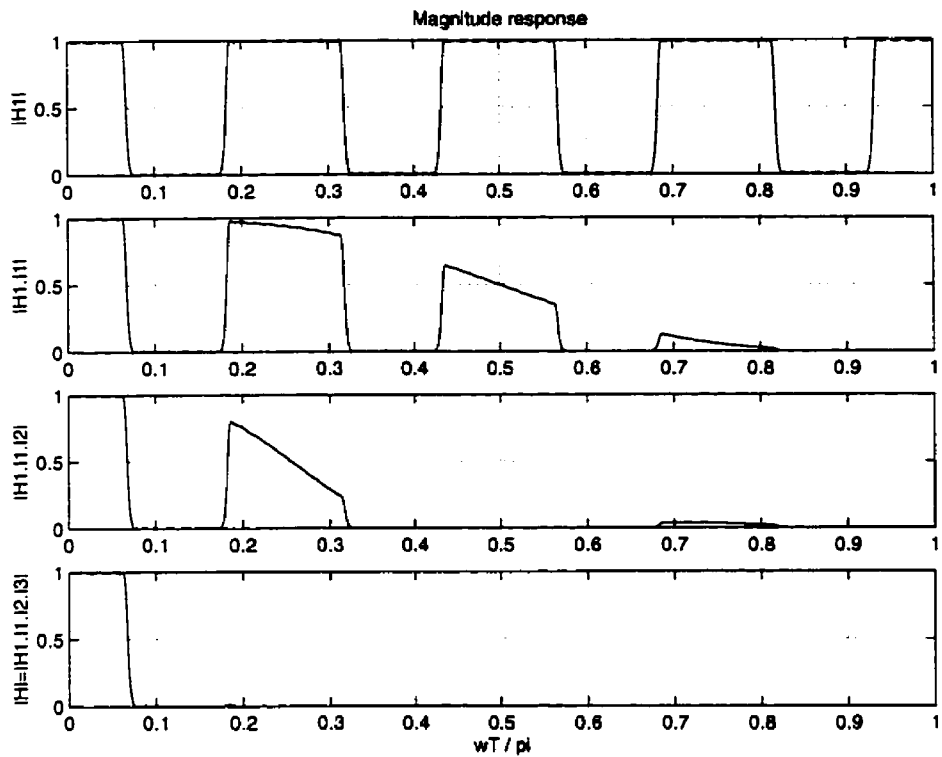


Fig.4.16(a) Magnitude response of model fitter, and cascade model filter with masking filters (for example 3).

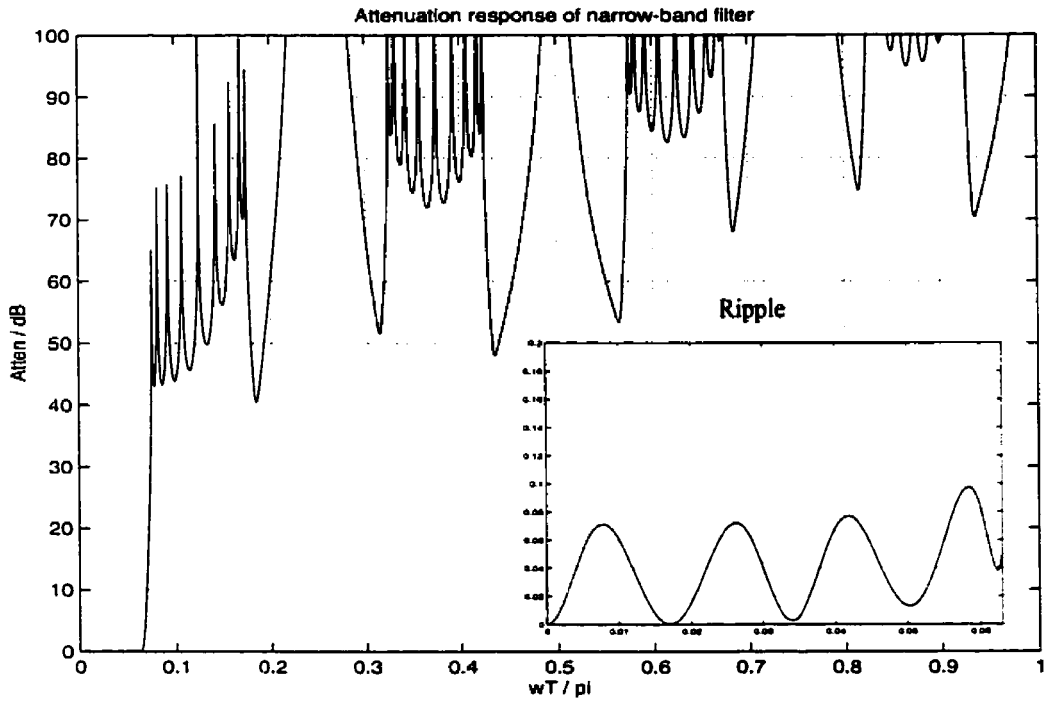


Fig. 4.16(b) Frequency response of overall narrow-band filter (example 3).

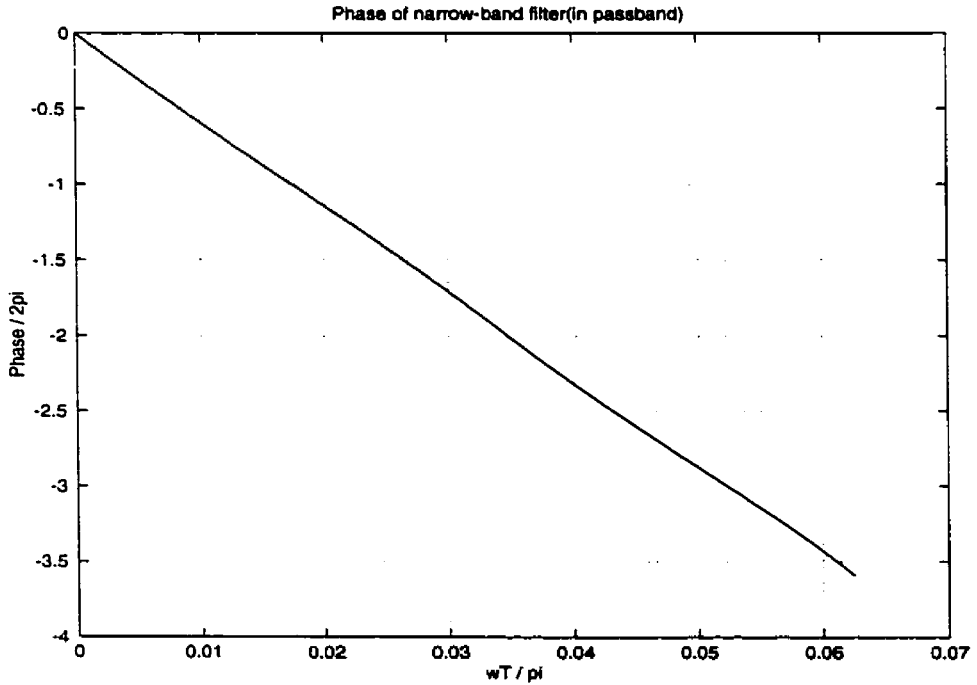


Fig. 4.16(c) Phase (in passband) response of overall narrow-band filter (example 3).

The corresponding wide-band filter can be obtained by using structure shown in Fig. 4.17.

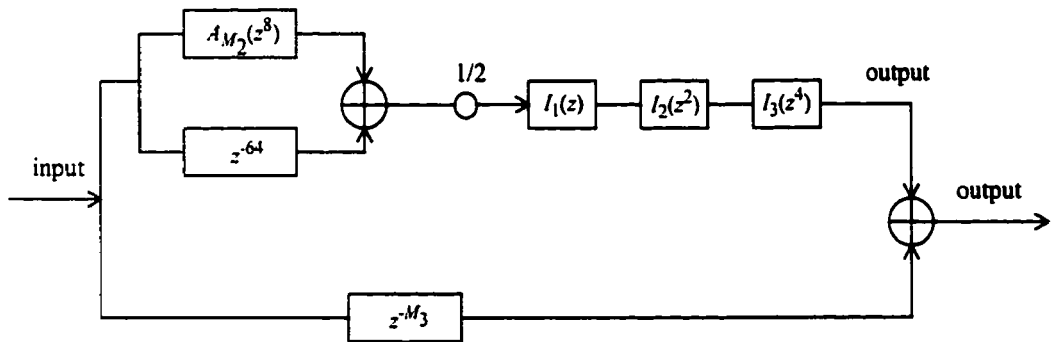


Fig. 4.17 Corresponding wide-band filter structure for example 3.

where

$$\begin{aligned}
 M_3 &= M \cdot M_1 + (K_1 + L_1 - 1) + 2(K_2 + L_2 - 1) + 4(K_3 + L_3 - 1) \\
 &= 8 \times 8 + 3 + 8 + 20 = 115
 \end{aligned}$$

The frequency response of corresponding wide-band filter is shown in Fig. 4.18.

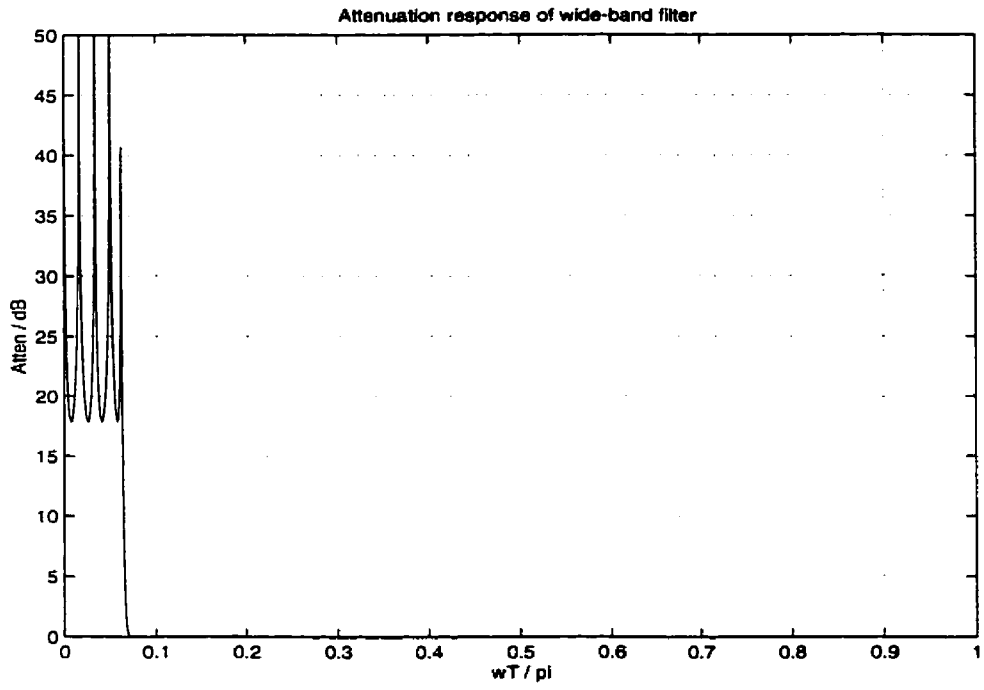


Fig. 4.18 The frequency response of corresponding wide-band filter for example 3.



# ***Chapter 5***

## ***Conclusions***

In this thesis, a method to design IIR multiple notch filters for a prescribed notch frequencies and 3 dB reflection bandwidths is discussed. This notch filter can be realized by a computationally efficient lattice structure with very low sensitivity. An example has been given to demonstrate the design procedure.

In the second part of this thesis, the design and realization methods for high speed narrow-band and wide-band filters have been given, the narrow-band filters are composed of a model filter and one or several masking filters in cascade. In the case of nonlinear phase, lattice and bireciprocal lattice WDFs are used for the model and masking filters; a conventional lattice WDF design method is given, a design method for bireciprocal WDFs is also given in detail. The wide-band filters consist of a narrow-band filter in parallel with one of the allpass filters. The overall narrow-band filters can be designed by separately designing the model filter and masking filters. The overall wide-band filters can be designed by first designing a narrow-band filter, then, by connecting this filter in parallel with an allpass filter consisting of a cascade of branches one from each subfilter of the narrow-band filter. Estimations were given for the passband and stopband ripples of the individual filters in the narrow-band filter in order to meet the requirements for the overall wide-band filter.

This offers simple design procedures for both narrow-band and wide-band filters since a conventional lattice WDF design method can be used. However, for many wide-band cases, these designs imply an unnecessarily high computational complexity, because the derived estimations are based on a worst case assumption. For the case of approximately linear phase, an approximately linear phase IIR filter is used for the model filter, and MF linear phase FIR filters are used for the masking filters. Because both cases (linear and nonlinear phase) are based on the interpolated technique, all recursive loops contain a number of delay elements, resulting in filters with higher maximal sample frequencies compared to the directly designed filters. We gave several examples to demonstrate the effects of quantization, the resulting filters have lower word-lengths compared with directly designed filters. We also discussed the roundoff noise and concluded that these filters are likely to be in favor.

## *Appendix*

### **1 Programs for multiple notch filters**

```
% program for multiple notch filters

clear;

format long;

% notch filter specification

order=6; %filter order

wN=[0.1*pi 0.4*pi 0.7*pi ]; % notch filter freq

bw=[0.01*pi 0.01*pi 0.02*pi]; % rejection bandwidth

%bw=[0.05*pi 0.05*pi 0.4*pi];

% calculate coefficients

for i=1:order

    w(i)=wN(floor((i+1)/2))-0.5*(1-(-1).^mod(i,2))*(bw(floor((i+1)/2))/2);

    phase(i)=-((2*(floor((i+1)/2))-1)*pi)+0.5*((1-((-1).^mod(i,2)))*pi/2);

    beta(i)=0.5*(phase(i)+order*w(i));

    tanb(i)=tan(beta(i));

    for k=1:order

        q(i,k)=sin(k*w(i))-(tanb(i))*(cos(k*w(i)));

    end

end

end
```

```

a=inv(q)*tanb';
disp('a='),disp(a),
g=[1 a.']; % in the z-domain
h=fliplr(g); % in the z-domain
[H,w] = freqz(h,g,1024);
figure(5)
phase = unwrap(angle(H));          % unwrapped phase
plot(w/pi,phase/pi);grid,xlabel('normalized frequency w / '), ylabel('phase / '),
title('phase of allpass'),
% calculate gammas
h=[1 a'];
g=[fliplr(a') 1];
n=length(g)-1;
gamma=zeros(1,n);
for i=1:n
    [gamma(i),h,g]=Exgamma(h,g);
end
disp('gamma='),disp(gamma)
% notch filter frequency response
M=512;% number of time instants
s=zeros(1,n); % initial state
input=zeros(1,2*order);
output=zeros(1,2*order);

```

```

b2=1;

%b2=data;

for m=1:M

    input(m)=b2;

    for i=1:n

        a1=b2;

        a2=s(i);

        [b1,b2]=Two_p_a(-gamma(i),a1,a2);

        if i>1

            s(i-1)=b1;

        else

            output(m)=b1;

        end

        if i==n

            s(i)=b2;

        end

    end % i-loop

b2=0;

end % m-loop

output=(output+input)*0.5;

t=linspace(0,M-1,M);

figure(2),stem(t,output),axis([0 100 -1 1]),grid, xlabel('discrete time n');

ylabel('h[n]'), title('Unit Sample Response');

```

```
% FFT of impulse response and plots of frequency responses
```

```
N=M;
```

```
y=fft(output,N);
```

```
x=linspace(0,1,N/2);
```

```
y1=[y(1:N/2)];
```

```
y2=abs(y1);
```

```
figure(3)
```

```
plot(x,y2),grid, xlabel('normalized frequency w / '), ylabel('|H|'),
```

```
title('Magnitude Response of IIR Multiple Notch Filter'),
```

```
figure(4)
```

```
om_index = 1:.99999*N/2+1;
```

```
om = x(om_index); % passband
```

```
phase1 = unwrap(angle(y1(om_index))); % unwrapped phase
```

```
plot(om,phase1);grid,xlabel('normalized frequency w / '), ylabel('phase / '),
```

```
title('phase of IIR Multiple Notch Filter')
```

```
%%%%%%%%%%%%%%%%%%%%%%%%%%%%%%%%%%%%%%%%%%%%%%%%%%%%%%%%%
```

```
function [gamma,h2,g2]=Exgamma(h1,g1)
```

```
gamma=polyval(h1,0)/polyval(g1,0);
```

```
h2=polyadd(h1,-gamma*g1);
```

```
m=length(h2);
```

```
h2(:,m)=[];
```

```
g2=polyadd(g1,-gamma*h1);
```

```
g2(:,1)=[];
```

```

%%%%%%%%%%%%%%%%%%%%%%%%%%%%%%%%%%%%%%%%%%%%%%%%%%%%%%%%%%%%%%%%%%%%%%%%
function [b1,b2]=Two_p_a(gamma,a1,a2)

b1=-gamma*a1+(1+gamma)*a2;

b2=a1*(1-gamma)+gamma*a2;

%%%%%%%%%%%%%%%%%%%%%%%%%%%%%%%%%%%%%%%%%%%%%%%%%%%%%%%%%%%%%%%%%%%%%%%%

```

```

function p=polyadd(a,b)

if nargin<2
    error('Not enough input arguments'),
end

a=a(:)';
b=b(:)';

na=length(a);
nb=length(b);

p=[zeros(1,nb-na) a] + [zeros(1,na-nb) b];

```

## 2 Programs for the wide-band filters

```

%example 2 for overall wide-band filter

%spec: wcT=0.075pi,wsT=0.0625pi,Ap<=0.2dB,As>=50dB high-pass

clear

format long

m=33;

b=zeros(1,m);

```

```

c1=zeros(1,11);c2=zeros(1,2);c3=zeros(1,1);c4=zeros(1,1);

d1=zeros(1,11);d2=zeros(1,5);d3=zeros(1,3);

e1=zeros(1,11);

output1=zeros(1,m);output2=zeros(1,m);output3=zeros(1,m);

%implement H1(z.^4) Amax=10.^(-5)db,Amin=40db,order=11
for n=0:4095

    a(6)=c1(3);c1(3)=d1(3);d1(3)=e1(3);e1(3)=b(6);%implement delays

    a(5)=c1(2);c1(2)=d1(2);d1(2)=e1(2);e1(2)=b(4);

    a1=a(5);

    a2=a(6);

    gamma=0.62686492810183;%Ap=10.^(-5),As=40db

    gamma=round(gamma*(2.^11))/(2.^11);

two_p_a1;

b(5)=b1;

b(6)=b2;

if n==0

    a(1)=1;

else

    a(1)=0;

end

a(2)=c1(1);c1(1)=d1(1);d1(1)=e1(1);e1(1)=b(2);

a1=a(1);

a2=a(2);

```



```

gamma=0.28671991154392;
gamma=round(gamma*(2.^11))/(2.^11);
two_p_al;
b(1)=b1;
b(2)=b2;
a(3)=b(1);
a(4)=b(5);
a1=a(3);
a2=a(4);
gamma=-0.53953031878987;
gamma=round(gamma*(2.^11))/(2.^11);
two_p_al;
b(3)=b1;
b(4)=b2;
a(10)=c1(5);c1(5)=d1(5);d1(5)=e1(5);e1(5)=b(10);
a(9)=c1(4);c1(4)=d1(4);d1(4)=e1(4);e1(4)=b(8);
a1=a(9);
a2=a(10);
gamma=0.66846224032534;
gamma=round(gamma*(2.^11))/(2.^11);
two_p_al;
b(9)=b1;
b(10)=b2;

```

```

a(8)=b(9);

a(7)=b(3);

a1=a(7);

a2=a(8);

gamma=-0.89502919636046;

gamma=round(gamma*(2.^11))/(2.^11);

two_p_a1;

b(7)=b1;

b(8)=b2;

a(14)=c1(7);c1(7)=d1(7);d1(7)=e1(7);e1(7)=b(14);

a(13)=c1(6);c1(6)=d1(6);d1(6)=e1(6);e1(6)=b(12);

a1=a(13);

a2=a(14);

gamma=0.57217228785650;

gamma=round(gamma*(2.^11))/(2.^11);

two_p_a1;

b(13)=b1;

b(14)=b2;

a(12)=b(13);

a(11)=a(1);

a1=a(11);

a2=a(12);

gamma=-0.24300630107066;

```

```

gamma=round(gamma*(2.^11))/(2.^11);

two_p_a1;

b(11)=b1;

b(12)=b2;

a(18)=c1(9);c1(9)=d1(9);d1(9)=e1(9);e1(9)=b(18);

a(17)=c1(8);c1(8)=d1(8);d1(8)=e1(8);e1(8)=b(16);

a1=a(17);

a2=a(18);

gamma=0.65574975306234;

gamma=round(gamma*(2.^11))/(2.^11);

two_p_a1;

b(17)=b1;

b(18)=b2;

a(15)=b(11);

a(16)=b(17);

a1=a(15);

a2=a(16);

gamma=-0.76476475528964;

gamma=round(gamma*(2.^11))/(2.^11);

two_p_a1;

b(15)=b1;

b(16)=b2;

a(22)=c1(11);c1(11)=d1(11);d1(11)=e1(11);e1(11)=b(22);

```

```

a(21)=c1(10);c1(10)=d1(10);d1(10)=e1(10);e1(10)=b(20);

a1=a(21);

a2=a(22);

gamma=0.67319504866259;

gamma=round(gamma*(2.^11))/(2.^11);

two_p_a1;

b(21)=b1;

b(22)=b2;

a(20)=b(21);

a(19)=b(15);

a1=a(19);

a2=a(20);

gamma=-0.97030342888112;

gamma=round(gamma*(2.^11))/(2.^11);

two_p_a1;

b(19)=b1;

b(20)=b2;

output1=b(19)+b(7);

%implement H2(z.^2)

a(26)=output1;

a(27)=d2(5);d2(5)=c2(2);c2(2)=d2(4);d2(4)=b(27);

a1=a(26);

a2=a(27);

```

```

gamma=-0.11455485826387;

gamma=round(gamma*(2.^11))/(2.^11);

two_p_al;

b(26)=b1;

b(27)=b2;

a(23)=d2(1);d2(1)=b(23);

b(23)=output1;

a(24)=a(23);

a(25)=d2(3);d2(3)=c2(1);c2(1)=d2(2);d2(2)=b(25);

a1=a(24);

a2=a(25);

gamma=-0.54458467232029;

gamma=round(gamma*(2.^11))/(2.^11);

two_p_al;

b(24)=b1;

b(25)=b2;

output2=b(24)+b(26);

%implement H20(z.^2) one allpass of H2(z.^2)

a(31)=d3(1);d3(1)=b(31);

b(31)=b(7);

a(32)=a(31);

a(33)=d3(3);d3(3)=c4(1);c4(1)=d3(2);d3(2)=b(33);

a1=a(32);

```

```

a2=a(33);

gamma=-0.54458467232029;%-0.488725856;

gamma=round(gamma*(2.^11))/(2.^11);

two_p_al;

b(32)=b1;

b(33)=b2;

%implement H3(z)

a(29)=output2;

a(30)=c3(1);c3(1)=b(30);

a1=a(29);

a2=a(30);

gamma=-0.3375033802279;%-0.308258011;

gamma=round(gamma*(2.^11))/(2.^11);

two_p_al;

b(29)=b1;

b(30)=b2;

a(28)=b(28);b(28)=output2-b(32)*(2.^3);

output3(n+1)=(a(28)+b(29))*((-2).^(-3));

end

x=0:4095;

figure(1)

stem(x,output3),grid,xlabel('n'),ylabel('h(n)'),title('Impulse Response'),

w=linspace(0,1,4096); %w is f/F

```

```

h=0;

for n=0:4095

    h=h+output3(n+1)*exp(w*(-n)*i*pi);

end

figure(2)

plot(w,abs(h)),grid, xlabel('wT / '), ylabel('|H|'),

title('magnitude response of overall wide-band filter'),

atten=-20*log10(abs(h));

figure(3)

plot(w,atten),axis([0 0.1 0 90]),grid, xlabel('wT / '), ylabel('dB'),

title('Attenuation response of overall wide-band filter'),

figure(4)

plot(w,atten),axis([0.07 1 -0.1 0.1]),grid, xlabel('wT / '), ylabel('dB'),

title('Attenuation response of overall wide-band filter'),

```

## ***References***

- [1] E. A. Guillemin, *Synthesis of Passive Networks*, Wiley, New York, 1957.
- [2] N. Balabanian, *Network Synthesis*, Prentice-Hall, Englewood Cliffs, N.J., 1958.
- [3] L. Weinberg, *Network Analysis and Synthesis*, McGraw-Hill, New York, 1962.
- [4] J. K. Skwirzynski, *Design Theory and Data for Electrical Filters*, Van Nostrand, London, 1965.
- [5] R. W. Daniels, *Approximation Methods for Electronic Filter Design*, McGraw-Hill, New York, 1974.
- [6] L. Gazsi, "Explicit formulas for lattice wave digital filters", *IEEE Trans. circuits and Syst.*, vol. CAS-32, pp. 68-88, Jan. 1985.
- [7] A. Antoniou, *Digital Filters: analysis, design, and applications*, Second Edition McGraw-Hill, Inc. New York, 1993.
- [8] A. Fettweis, "Digital filter structures related to classical filter networks", *Arch. Elek. Uebertragung*, vol. 25, pp. 79-89, Feb. 1971,
- [9] A. Fettweis, H. Levin, and A. Sedlmeyer, "Wave digital lattice filters", *Int. J. Circuit Theory Appl.*, vol. 2, no. 2, pp. 203-211, June 1974.
- [10] V. Belevitch, *Classical Network Theory*, San Francisco, CA: Holden-day, 1968.
- [11] A. Fettweis, "Scattering properties of real and complex lossless two-ports", *Proc. IEEE*, vol. 128, Pt. G, No. 4, Aug. 1981.
- [12] A. Fettweis, "Digital filter structures related to classical filter networks", *Arch. Elek. Uebertragung*, vol 25, PP. 79-89, Feb. 1971.



- [13] S. Darlington, "Simple algorithms for elliptic filters and generalizations thereof", IEEE Trans. Circuits Syst., vol. CAS-25, pp. 975-980, Dec. 1978.
- [14] W. Wegener, "Wave digital directional filters with reduced number of multipliers and adders", Arch. Elek. Uebertragung., vol. 33, pp. 239-243, June. 1979.
- [15] S. C. Pei and C. C. Tseng, "IIR multiple notch filter design based on allpass filter", IEEE Trans. Circuits Syst. II, vol. 44, PP. 133-136, Feb. 1997.
- [16] X. Zhang and H. Iwakura, "Novel method for designing digital allpass filters based on eigenvalue problem", Electron. Lett., vol. 29, no. 14, pp. 1279-1281, July 1993.
- [17] G. O. Martens, Private communication.
- [18] Y. Neuvo, C. Y. Dong, and S. K. Mitra, "Interpolated finite impulse response filters", IEEE Trans. on Acoust, Speech and Signal Proc, vol. ASSP-32, pp. 563-570, June 1984.
- [19] T. Saramaki, Y. Neuvo, and S. K. Mitra, "Design of computationally efficient interpolated FIR filters", IEEE Trans. Circuits Syst., vol. 35, pp. 70-88, Jan. 1988.
- [20] H. Johansson, and L. Wanhammar, "Wave Digital Filter Structures for High-Speed Narrow-Band Filtering", IEEE Trans on circuits and systems II, June 1999.
- [21] M. Renfors and Y. Neuvo, "The maximum sampling rate of digital filters under hardware speed constraints", IEEE Trans. Circuits Syst., vol. CAS-28, pp. 196-202, Mar. 1981.
- [22] A. P. Chandrakasan and R. W. Brodersen, *Low Power Digital CMOS Design*. Norwell, MA: Kluwer, 1995.
- [23] M. Vesterbacka, "On implementation of maximally fast wave digital filters", dissertation no. 487, Linkoping Studies in Science and Technology, Linkoping Univ., Swe-

- den, 1997.
- [24] M. Vesterbacka, K. Palmkvist, P. Sandberg, and L. Wanhammar, "Implementation of maximally fast bit-serial lattice wave digital filters", in *proc. IEEE Int. Symp. Circuits and Systems, ISCAS'94, London, U.K., vol. 1, pp. 113-116.*
  - [25] J. Chung, H. Kim, and K. K. Parhi, "Pipelined lattice WDF design for wide-band filters", *IEEE Trans. on Circuits and Systems II*, vol. 42, No. 9, Sep 1995.
  - [26] M. Renfors and T. Saramaki, "A class of approximately linear phase digital filters composed of allpass subfilters", in *Proc. 1986 IEEE ISCAS, pp. 678-681, San Jose, CA, May 1986.*
  - [27] P. P. Vaidyanathan, "Efficient and Multiplierless Design of FIR Filters with Very Sharp Cutoff via Maximally Flat Building Blocks", *IEEE Trans on circuits and systems*, vol. CAS-32, No. 3, pp. 236-244, Mar. 1985.
  - [28] J. F. Kaiser, "Design subroutine (MXFLAT) for symmetric FIR lowpass digital filters with maximally flat pass and stop bands", in *Programs for digital signal processing*, New York: IEEE Press, 1979.
  - [29] A. V. Oppenheim and R. Schaffer, *Digital Signal Processing*. Addison Wesley, 1987.
  - [30] J. G. Chung and K. K. Parhi, "Pipelined wave digital filter design for narrow-band sharp transition digital filters", in *Proc. 1994 IEEE Wkshp. VLSI Signal Process., La Jolla, CA, Oct. 1994, pp. 501-510.*
  - [31] A. Fettweis, "Wave digital filters: Theory and practice", *Proc. IEEE*, vol. 74, PP. 270-327, Feb. 1986.
  - [32] J. G. Chung and K. K. Parhi, *Pipelined Lattice and Wave digital Recursive Filters*. Norwell, MA: Kluwer, 1996.